Palaeogeography, Palaeoclimatology, Palaeoecology 591 (2022) 110876

Contents lists available at ScienceDirect

Palaeogeography, Palaeoclimatology, Palaeoecology

journal homepage: www.elsevier.com/locate/palaeo

Refined geochronology and revised stratigraphic nomenclature of the Upper Cretaceous Wahweap Formation, Utah, U.S.A. and the age of early Campanian vertebrates from southern Laramidia

Tegan L. Beveridge [a,*], Eric M. Roberts [a], Jahandar Ramezani [b], Alan L. Titus [c], Jeffrey G. Eaton [d,e], Randall B. Irmis [e,f], Joseph J.W. Sertich [g,h]

[a] Department of Earth and Environmental Science, James Cook University, Townsville, QLD 4811, Australia
[b] Department of Earth, Atmospheric and Planetary Science, Massachusetts Institute of Technology, Cambridge, MA 02139, USA
[c] Paria River District, Bureau of Land Management, Kanab, UT 84741, USA
[d] P.O. Box 231, Tropic, UT 84776, USA
[e] Natural History Museum of Utah, University of Utah, Salt Lake City, UT 84108-1214, USA
[f] Department of Geology & Geophysics, University of Utah, Salt Lake City, UT 84112-0102, USA
[g] Department of Earth Sciences, Denver Museum of Nature and Science, Denver, CO 80205, USA
[h] Department of Geosciences, Warner College of Natural Resources, Colorado State University, Fort Collins, CO 80523, USA

ARTICLE INFO

Editor: Howard Falcon-Lang

Keywords:
Stratigraphy
Member
High-precision
CA-ID-TIMS
Age-stratigraphic model
Paleontology

ABSTRACT

The Western Interior of North America preserves one of the most complete successions of Upper Cretaceous marine and non-marine strata in the world; among these, the Cenomanian-Campanian units of the Kaiparowits Plateau in southern Utah are a critical archive of terrestrial environments and biotas. Here we present new radioisotopic ages for the Campanian Wahweap Formation, along with lithostratigraphic revision, to improve the geological context of its fossil biota. The widely accepted informal stratigraphic subdivisions of the Wahweap Formation on the Kaiparowits Plateau are herein formalized and named the Last Chance Creek Member, Reynolds Point Member, Coyote Point Member, and Pardner Canyon Member (formerly the lower, middle, upper, and capping sandstone members respectively). Two high-precision U-Pb zircon ages were obtained from bentonites using CA-ID-TIMS, supported by five additional bentonite and detrital zircon LA-ICP-MS ages. Improved geochronology of the Star Seep bentonite from the base of the Reynolds Point Member via CA-ID-TIMS demonstrates that this important marker horizon is over a million years older than previously thought. A Bayesian age-stratigraphic model was constructed for the Wahweap Formation using the new geochronologic data, yielding statistically robust ages and associated uncertainties that quantifiably account for potential variations in sediment accumulation rate. The new chronostratigraphic framework places the lower and upper formation boundaries at 82.17 +1.47/-10.63 Ma and 77.29 +0.72/-0.62 Ma, respectively, thus constraining its age to the first half of the Campanian. Additionally, a holistic review of known vertebrate fossil localities from the Wahweap Formation was conducted to better understand their spatio-temporal distribution including revised ages for early members of iconic dinosaur lineages such as Tyrannosauridae, Hadrosauridae, and Centrosaurinae. Chrono- and lithostratigraphic refinement of the Wahweap Formation and its constituent biotic assemblages establishes an important reference for addressing questions of Campanian terrestrial paleoecology and macroevolution, including dinosaur endemism and diversification throughout western North America.

1. Introduction

The Western Interior of North America preserves near-continuous successions of Upper Cretaceous strata deposited in a variety of settings ranging from alluvial and lacustrine to epicontinental marine (e.g., Molenaar and Rice, 1988; Kauffman, 1985; Roberts and Kirschbaum, 1995; Miall et al., 2008). These world-famous strata have been instrumental in developing global concepts of Cretaceous geochronology,

* Corresponding author at: C.O. EGRU, 1 James Cook Drive, Douglas, QLD 4811, Australia.
E-mail address: tegan.beveridge@my.jcu.edu.au (T.L. Beveridge).

https://doi.org/10.1016/j.palaeo.2022.110876
Received 5 July 2021; Received in revised form 3 February 2022; Accepted 6 February 2022
Available online 10 February 2022

biochronology, sequence stratigraphy, paleoclimatology, and paleontology (e.g., van Wagoner and Bertram, 1995; Lehman, 1997; Cifelli et al., 2004; Cobban et al., 2006; Fricke et al., 2010; Sampson et al., 2010; Loewen et al., 2013a; Sewall and Fricke, 2013; Titus and Loewen, 2013; Voris et al., 2020; Wilson et al., 2020). Among these strata, the Upper Cretaceous succession of the Kaiparowits Plateau in southern Utah, U.S.A., preserves one of the most complete non-marine records in the Western Interior, and is remarkable for its abundant and diverse floral, invertebrate, and vertebrate fossil contents (e.g., Titus and Loewen, 2013, and papers therein). These strata include the coastal to fluvial upper Turonian to Santonian Straight Cliffs Formation, fluvial lower to middle Campanian Wahweap Formation, and fluvial middle to upper Campanian Kaiparowits Formation. Fossils from these formations have been particularly important for developing recent hypotheses on the biogeographic distribution and macroevolution of Late Cretaceous dinosaurs and other non-marine tetrapods in western North America (e.g., Sankey, 2001; Gates et al., 2010; Sampson et al., 2010; Loewen et al., 2013a; Voris et al., 2020). Rigorous investigation of these hypotheses of latitudinal endemism across Laramidia, the western of the two North American landmasses separated by the Western Interior Seaway during the Cretaceous (Fig. 2), requires temporally calibrated contemporaneous biota from both northern and southern localities (Sampson et al., 2010).

Paleontological research in the Wahweap Formation in southern Utah over the last 30 years has documented a wealth of fossil taxa comprising significant Campanian non-marine assemblages from southern Laramidia (e.g., Cifelli, 1990a, 1990b, 1990c; Eaton, 1991, 2002; Eaton et al., 1999a, 1999b; Kirkland and DeBlieux, 2010; Gates et al., 2011, 2014; Loewen et al., 2013a; Titus and Loewen, 2013, and papers therein; Holroyd and Hutchison, 2016; Lund et al., 2016; Titus et al., 2016). Indeed, because fossil exploration in the formation began relatively recently, compared to historic work from northern Laramidia, the paleontological significance of the Wahweap Formation is only now becoming more widely recognized. An exceptionally diverse microfaunal assemblage and an ever-increasing collection of larger taxa from the formation, including some of the earliest known members of dominant Late Cretaceous dinosaur lineages such as Tyrannosauridae, Hadrosauridae, and Centrosaurinae (e.g., Kirkland and DeBlieux, 2010; Loewen et al., 2013a; Gates et al., 2014; Lund et al., 2016), highlight the need to place these important fossils in a more refined temporal context.

The lithostratigraphic framework for the Wahweap Formation proposed by Eaton (1991), including informal member subdivisions on the Kaiparowits Plateau, has proven to be widely accepted and practical through repeated use in all subsequent sedimentological and paleontological studies. The age of the Wahweap Formation, indicated by Eaton (1991) as early Campanian based on mammal biostratigraphy, was later investigated by Jinnah et al. (2009) and Jinnah (2013) using $^{40}Ar/^{39}Ar$ geochronology from two interstratified bentonite (weathered volcanic ash) beds. These, along with two U-Pb detrital zircon maximum depositional ages (Jinnah et al., 2009) remain the only documented radioisotopic age constraints for the Wahweap Formation; however, subsequent magnetostratigraphic analysis (Albright and Titus, 2016) suggested that these early radioisotopic dates were erroneously young, leading to ambiguity about the formation's true age.

The purpose of this study is to 1) formalize lithostratigraphic nomenclature for the Wahweap Formation; 2) provide new U-Pb zircon ages underpinned by high-precision chemical abrasion isotope dilution thermal ionization mass spectrometry (CA-ID-TIMS) for the Star Seep bentonite and supported by additional laser ablation inductively coupled plasma mass spectrometry (LA-ICP-MS) bentonite zircon and detrital zircon ages; 3) establish a well-resolved chronostratigraphic framework in the form of a Bayesian age-stratigraphic model for the formation; and 4) integrate the new temporal framework for the Wahweap Formation with its vertebrate fossil content.

Resolving the temporal framework of the Wahweap Formation and refining lithostratigraphic subdivisions within which paleontological specimens are placed provides much needed chronostratigraphic clarity. This can be used for subsequent paleoecological and evolutionary studies and elucidates the age of key vertebrate taxa for understanding classic Campanian-Maastrichtian non-marine ecosystems from western North America. Furthermore, our work advocates for best practice age reporting, specifically regarding the inclusion of uncertainty, which is often unreported and becomes statistically significant in studies that investigate geologically rapid evolutionary processes such as taxal turnovers and diversification. Outcomes from our work support ongoing investigations of hypothesized Late Cretaceous latitudinal biotic distributions in North America and the driving mechanisms behind species diversification intervals leading to the 'zenith of the dinosaurs' (Sloan, 1976; Dodson, 1983; Clemens, 1986; Dodson and Tatarinov, 1990) in the Campanian and Maastrichtian.

2. Previous work

2.1. Lithostratigraphy

The Wahweap Formation, first described by Gregory and Moore (1931) as the Wahweap Sandstone, is a 360 to 460-m-thick fluvial succession comprising interbedded floodplain mudstones and channel sandstones. Peterson and Waldrop (1965) formally defined the unit as the Wahweap Formation, which was followed by more detailed sedimentological investigation by Peterson (1969), Eaton (1991), Little (1995), Pollock (1999), Simpson et al. (2008, 2014) and Jinnah and Roberts (2011). The Wahweap Formation is exposed in southern Utah, U.S.A., along the margins of the Markagunt and Paunsaugunt plateaus (Biek et al., 2015) and extensively throughout the Kaiparowits Plateau (Fig. 1) and is also correlated to the Masuk and Tarantula Mesa Sandstone formations to the northeast in the nearby Henry Basin (Eaton, 1990; Corbett et al., 2011; Jinnah, 2013; Lawton et al., 2014a). These four physiographic regions were partitioned by the (west to east) Hurricane, Sevier, and Paunsaugunt faults, and the East Kaibab and Waterpocket monoclines (Fig. 2) (Titus et al., 2013). Although all contain exposures of Upper Cretaceous strata, the Kaiparowits Plateau preserves the most numerous Wahweap Formation fossil localities of the four areas. This observed distribution potentially represents discovery bias due to the nature of exposures on the Kaiparowits Plateau as opposed to the heavily forested and inaccessible Markagunt and Paunsaugunt plateaus (the latter hosts rich microvertebrate localities, e.g., Eaton, 1999; Eaton and Cifelli, 2013; Titus et al., 2016); however, it nevertheless highlights the need for targeted chronostratigraphic work on the heavily studied, fossiliferous Kaiparowits Plateau exposures east of the East Kaibab Monocline.

Two models for lithostratigraphic subdivision of the Wahweap Formation have previously been proposed. Eaton (1991) proposed the subdivisions of lower, middle, upper and capping members (informal) based largely on sand:mud ratios and changes in alluvial architecture observed on the Kaiparowits Plateau. Doelling (1997), on the other hand, described outcrops from the Markagunt and Paunsaugunt plateaus and did not delineate the lower three units of Eaton (1991); recommending instead only a lower and upper unit where Doelling's upper unit correlated to Eaton's capping sandstone. Discrepancies in sedimentary architecture of the lower portion of the formation across the three southern Utah plateaus and the Henry Basin succession are attributed to lateral facies change from proximal to distal floodplain environments (Corbett et al., 2011; Jinnah and Roberts, 2011). Due to this lateral variation in sedimentological character, our lithostratigraphic and geochronologic study is generally restricted to strata across the Kaiparowits Plateau region.

2.2. Chronostratigraphy

The Wahweap Formation has previously been constrained as early to middle Campanian in age based on biostratigraphic and radioisotopic

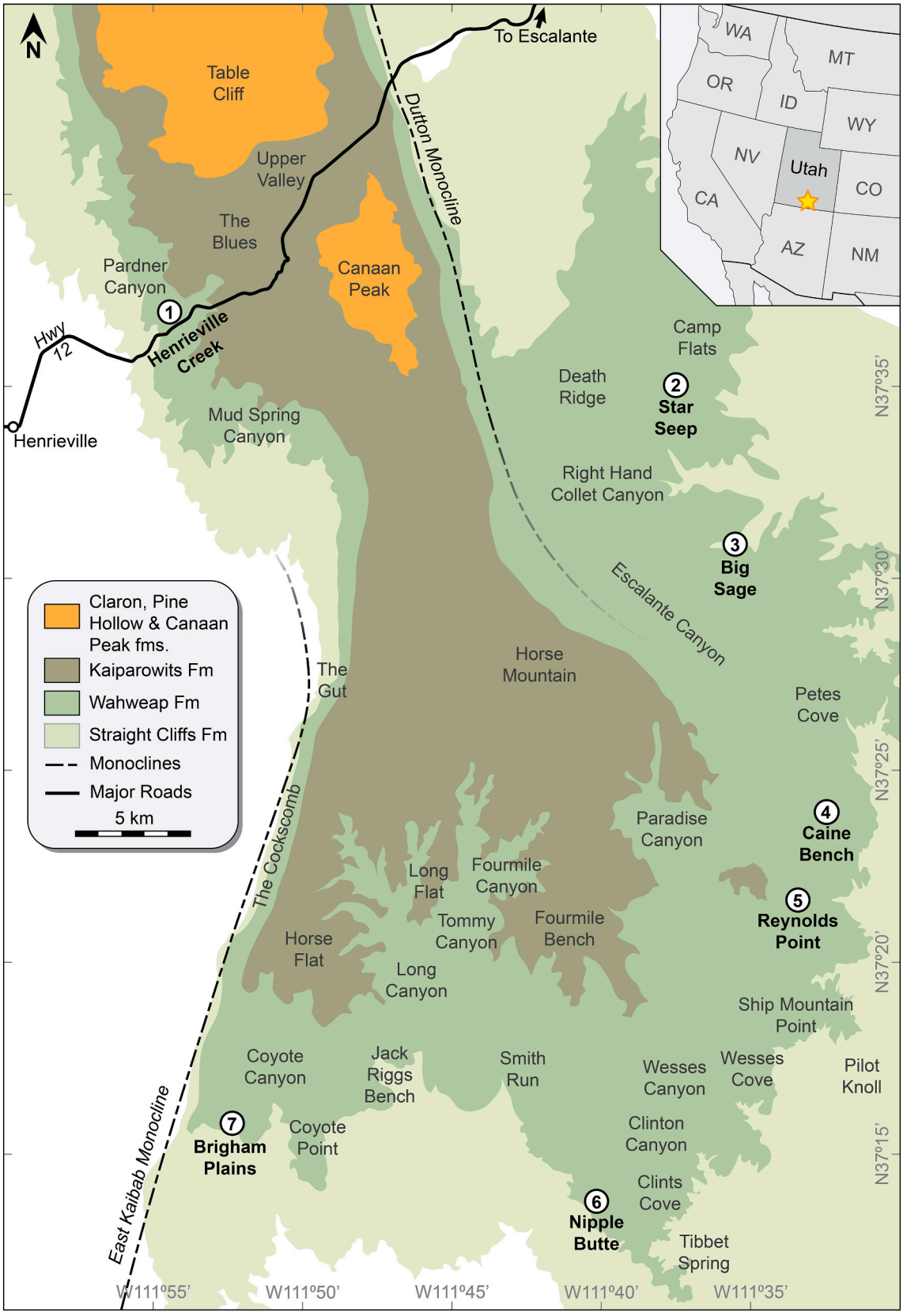

Fig. 1. Simplified geological map of the Kaiparowits Plateau, including field area names, compiled from various USGS 1:24,000 and the USGS 1:100,000 geological maps of the Escalante and Smoky Mountain 30′ x 60′ quadrangles by Doelling and Willis (2006, 2018). Numbers refer to measured stratigraphic sections in Fig. 4.

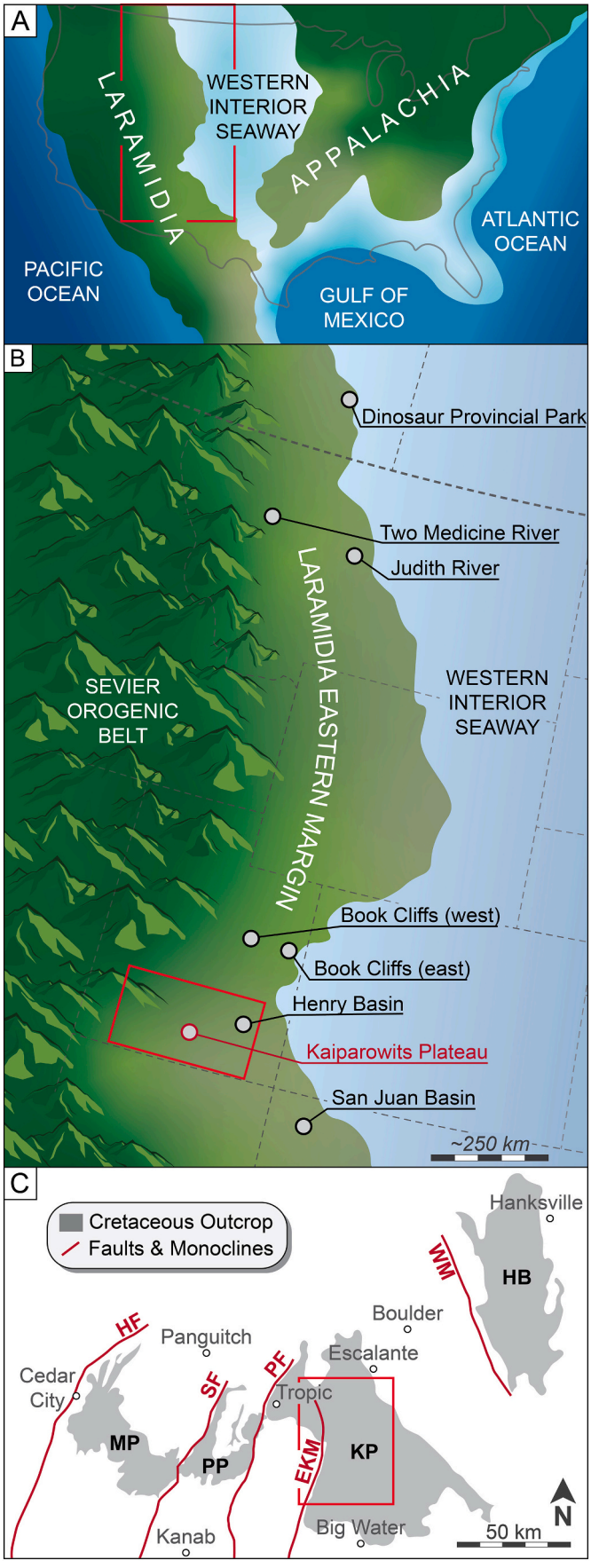

(caption on next column)

Fig. 2. Large-scale palaeogeographic and physiographic maps illustrating the relative position of the Kaiparowits Plateau. A) Continental paleogeography at ca 80 Ma illustrating western (Laramidia) and eastern (Appalachia) North America separated by the Western Interior Seaway (red box = panel B; adapted from Sampson et al., 2010, and references therein). B) Interpreted paleogeography of central-eastern Laramidia at ca 80 Ma illustrating the relative positions of key areas with early Campanian strata (see Fig. 9) (red box = panel C; adapted from Lehman, 1997, Jinnah et al., 2009 and Titus et al., 2013). C) Southern Utah physiographic regions illustrating the Markagunt (MP), Paunsaugunt (PP) and Kaiparowits (PP) plateaus and the Henry Basin (HB), partitioned by structural features including the Hurricane (HF), Sevier (SF) and Paunsaugunt (PF) faults and the East Kaibab (EKM) and Waterpocket (WM) monoclines (red box = Fig. 1; adapted from Titus et al., 2013). (For interpretation of the references to color in this figure legend, the reader is referred to the web version of this article.)

dating methods, additionally supported by magnetostratigraphic and sequence stratigraphic inferences (Eaton, 1991; Jinnah et al., 2009; Jinnah and Roberts, 2011; Eaton and Cifelli, 2013; Albright and Titus, 2016). Detailed biostratigraphic efforts over the years include meticulous vertebrate microfossil work, particularly on mammaliaform assemblages, which suggested an early to middle Campanian age for the Wahweap Formation (Eaton, 1991, 1999, 2002; Eaton et al., 1999a, 1999b; Eaton and Cifelli, 2013). Alluvial sequence stratigraphic studies of the Wahweap Formation have identified a sequence boundary at the top of the Coyote Point Member (formerly the upper member), inferred to reflect the globally recognized ~80 Ma sequence boundary (Lawton et al., 2003; Jinnah and Roberts, 2011; Haq, 2014). Although these studies provided useful age control, independent radioisotopic geochronology is required to construct a robust chronostratigraphic framework for the Wahweap Formation at the resolution necessary for more detailed paleoecological work. Despite their inherent intricacies (see Bowring et al., 2006), radioisotopic chronometers provide the only means of arriving at a numerical age that can be globally correlated. Additionally, a biostratigraphically-independent geochronologic framework avoids circular interpretations when trying to simultaneously indicate age and infer biogeographic and macroevolutionary patterns from the same fossil assemblage (e.g., Irmis et al., 2010).

Jinnah et al. (2009) published the first radioisotopic age data for the Wahweap Formation, including an $^{40}Ar/^{39}Ar$ bentonite age from ~40 m above the base of the formation in the Camp Flat area (Fig. 1), as well as two U-Pb detrital zircon maximum depositional ages generated using the sensitive high resolution ion microprobe (SHRIMP) technique (Jinnah et al., 2009). Using these data and other $^{40}Ar/^{39}Ar$ ages from the overlying Kaiparowits Formation that provide minimum age constraint (Roberts et al., 2005), Jinnah et al. (2009) extrapolated a linear average sediment accumulation rate of between 8.4 and 13.1 cm/ka for the Wahweap Formation. The initial bentonite age was later recalculated (Jinnah, 2013) using the revised age of the Fish Canyon Tuff sanidine standard of 28.2 Ma (Kuiper et al., 2008). The recalculated bentonite age of 80.6 ± 0.6 Ma (2σ internal error) was also accompanied by a second radioisotopically dated bentonite reportedly ten meters higher in section from the adjacent Star Seep area. The latter sample yielded an $^{40}Ar/^{39}Ar$ age of 79.9 ± 0.6 Ma. From this work, the Wahweap Formation was estimated to have been deposited between 81 and 77 Ma (Jinnah et al., 2009; Jinnah, 2013).

The above two $^{40}Ar/^{39}Ar$ bentonite ages remained for nearly a decade the only absolute constraints on the Wahweap Formation, whose abundance of well-preserved bentonites is significantly lower than that of the overlying Kaiparowits Formation. More recent magnetostratigraphic work by Albright and Titus (2016) identified a polarity reversal attributed to the C33r-C33n chron boundary 200 m stratigraphically higher than the upper bentonite of Jinnah (2013); however, both the reversal and the bentonite were thought to be ~79 Ma given the then-current calibrations (GTS2012 – Ogg, 2012; Jinnah, 2013). To rectify this discrepancy, Albright and Titus (2016) revisited the calibration of

the C33r-C33n reversal based on $^{40}Ar/^{39}Ar$ geochronology of its reference section in the Elk Basin, Wyoming, and suggested a new age for this magnetochron boundary of 78.91 Ma, although this change was not adopted in GTS2020 (Gradstein et al., 2020). Findings from Albright and Titus (2016) thus also highlighted the need for more robust of radioisotopic ages from the Wahweap Formation and across the Western Interior.

Chronostratigraphic divisions and nomenclature used in this study reflect globally recognized definitions described in GTS2020 (Gradstein et al., 2020). Thus, the Campanian stage is constrained to between 83.6 (±0.2) Ma and 72.1 (±0.2) Ma, and further chronostratigraphic subdivision is not formally recognized (see Gale et al., 2020). In North America, informal early, middle, and late Campanian subdivisions are common and although these constitute useful signposts, strict adherence to numerical boundary ages for these subdivisions represents a greater degree of confidence in these definitions than is currently appropriate. As such, the terms early and middle Campanian are used in this study to generally match a transition at ca 80.6 Ma indicated by the global first occurrence of *Baculites obtusus* in the marine realm (Cobban et al., 2006; Gale et al., 2020), although numerical ages are considered more relevant than the relative early and middle Campanian assignments.

2.3. Paleontology

Nearly one hundred aquatic and terrestrial vertebrate taxa have been recovered from the Wahweap Formation, making it one of the most diverse early to middle Campanian assemblages in North America (Eaton, 1999; Eaton et al., 1999a, 1999b; DeBlieux et al., 2013; Titus and Loewen, 2013, and papers within; Titus et al., 2016). These assemblages includes hadrosaurid, ceratopsid, and rare pachycephalosaurid and ankylosaurian ornithischian dinosaurs; tyrannosaurid and maniraptoran theropod dinosaurs; as well as numerous taxa of freshwater sharks and rays (chondrichthyans), bony fish (actinopterygians), lissamphibians (frogs, salamanders, and albanerpetontids), turtles, crocodyliforms, squamates (lizards), and many mammaliaforms (Cifelli, 1990a, 1990b, 1990c; Eaton, 1991, 2002; Eaton et al., 1999a, 1999b; Kirkland and DeBlieux, 2010; Gates et al., 2011, 2014; Brinkman et al., 2013; DeBlieux et al., 2013; Gardner et al., 2013; Eaton and Cifelli, 2013; Irmis et al., 2013; Kirkland et al., 2013; Loewen et al., 2013a, 2013b, 2013c; Roček et al., 2013; Holroyd and Hutchison, 2016; Lund et al., 2016; Titus et al., 2016) (see Supplementary material 1). Fossil material ranges from associated skeletons to isolated skeletal elements, teeth, osteoderms, fish scales, decapod crustacean claws, mollusk shells, petrified wood, leaves, and rare coprolites. Many of these smaller fossils occur commonly in micro- and mesovertebrate channel lag deposits in the lower three units of the formation (Jinnah and Roberts, 2011; DeBlieux et al., 2013; Supplementary material 1). Although relatively common in the overlying Kaiparowits Formation, articulated and associated remains in overbank mudstone deposits are less common in the Wahweap Formation (DeBlieux et al., 2013), though this may be a stochastic sampling effect of fewer recorded vertebrate sites overall and increased reconnaissance efforts have begun to reveal more localities. A number of tetrapod trackways have been identified in the Wahweap Formation, particularly within strata at the boundary between the Last Chance Creek and Reynolds Point members (formerly lower and middle members), which predominantly preserve tridactyl impressions from hadrosaurs but also contain quadrupedal and smaller bipedal tracks possibly left by ceratopsians and theropods respectively (Hamblin and Foster, 2000; DeBlieux et al., 2013).

Though the diverse faunal assemblage of the Wahweap Formation is known mostly from microsites (fragments <10 cm), and many taxa require more complete skeletal material for detailed identification and phylogenetic placement, notable macrofossils include early representatives of iconic latest Cretaceous dinosaur lineages such as the tyrannosaurid *Lythronax argestes* (Loewen et al., 2013a), the centrosaurine ceratopsids *Diabloceratops eatoni* (Kirkland and DeBlieux, 2010) and *Machairoceratops cronusi* (Lund et al., 2016), and the hadrosaurids *Adelolophus hutchisoni* (Gates et al., 2014), *Acristavus gagslarsoni* (Gates et al., 2011) and two additional unnamed taxa (Gates et al., 2014). These terrestrial large-bodied taxa, all described within the last decade, are part of critical early to middle Campanian assemblages from southern Laramidia including the potentially oldest known members of Tyrannosauridae, Hadrosauridae, and Ceratopsidae (Kirkland and DeBlieux, 2010; Loewen et al., 2013a; Gates et al., 2014; Holroyd and Hutchison, 2016; Voris et al., 2020; Wilson et al., 2020). As such, precise chronostratigraphic context of these biotic assemblages is a crucial component for continental-scale paleoecological hypotheses around dinosaur diversification and endemism during the Late Cretaceous (e.g., Sankey, 2001; Gates et al., 2010; Sampson et al., 2010; Loewen et al., 2013a; Voris et al., 2020).

3. Lithostratigraphic nomenclature of the Wahweap Formation

Given the high degree of acceptance of the informal lithostratigraphic subdivisions specified for the Wahweap Formation by Eaton (1991), we propose formalization of these members on the Kaiparowits Plateau following the guidelines of the International Commission on Stratigraphy and the North American Stratigraphic Code (see Oriel et al., 2005). Formalization will significantly aid in clear and consistent reporting of fossil resources from the formation and simplify future stratigraphic studies. In place of the informal lower, middle, upper, and capping sandstone units of the Wahweap Formation on the Kaiparowits Plateau proposed by Eaton (1991), we suggest the names Last Chance Creek Member, Reynolds Point Member, Coyote Point Member, and Pardner Canyon Member, respectively. Examples of these formal subdivisions are annotated on field photographs from exposures on the southern Kaiparowits Plateau in Fig. 3 and boundary ages are listed in Table 2. We see the application of the lower three formal members as generally restricted to the Kaiparowits Plateau, whereas exposures on the Markagunt and Paunsaugunt plateaus should continue to be referred to as undifferentiated Wahweap Formation. The Pardner Canyon Member (previously capping sandstone member) is found extensively across all three plateaus (Biek et al., 2015) and is confidently correlated with the Tarantula Mesa Sandstone in the Henry Basin (Eaton, 1990; Jinnah et al., 2009; Corbett et al., 2011). All four members of the Wahweap Formation have been described in detail by Eaton (1991), Jinnah and Roberts (2011) and many others; thus, the following descriptions are a synthesis of previous work paired with observations from our study.

3.1. Last Chance Creek Member

The Last Chance Creek Member (formerly the lower member) begins at the first major mudstone horizon above the Drip Tank Member of the Straight Cliffs Formation and is 65 m thick at the Reynolds Point lectostratotype section (Eaton, 1991; Jinnah and Roberts, 2011). The lower contact represents a notable depositional hiatus, identified by the coincidence of the C34n-C33r paleomagnetic reversal boundary (Albright and Titus, 2016), and a sharp paraconformity across much of the Kaiparowits Plateau. The northward thinning Last Chance Creek Member ranges in thickness from 20 to 65 m and is mudstone dominated, although sandier in the north, and contains several laterally continuous single-story cross-bedded sandstone channel deposits including a distinctive bench-forming sandstone that caps the unit (Eaton, 1991; this study). The name Last Chance Creek is derived from the so-named watercourse adjacent to the Reynolds Point lectostratotype section measured by Eaton (1991) and proximal to the holotype locality of the ceratopsid dinosaur *Diabloceratops eatoni* (Kirkland and DeBlieux, 2010).

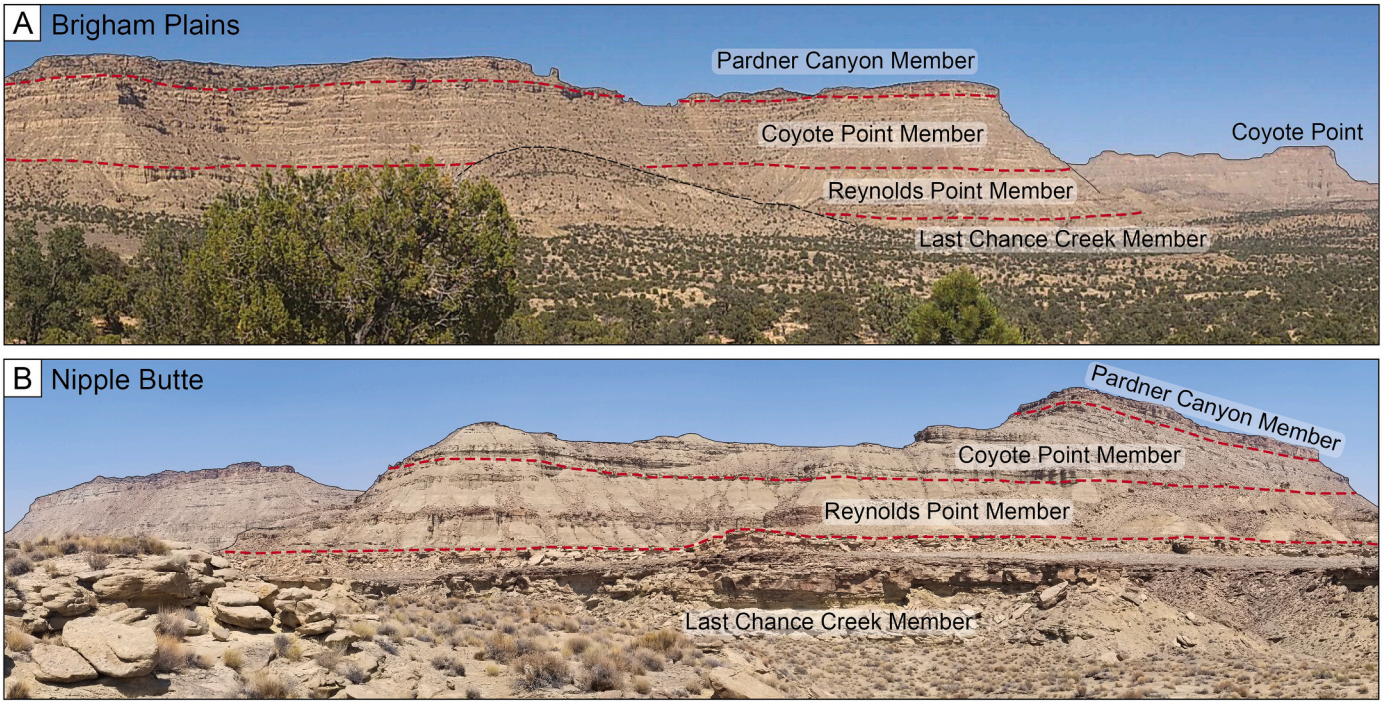

Fig. 3. Exposures of the Wahweap Formation on the southern flank of the Kaiparowits Plateau where partial stratigraphic sections were measured at A) Brigham Plains, and B) Nipple Butte, illustrating the new member nomenclature.

3.2. Reynolds Point Member

The Reynolds Point Member (formerly the middle member) is 112 m thick at Reynolds Point and is commonly recessive above the Last Chance Creek Member, containing a higher proportion of floodplain deposits than the underlying member, and friable fine-grained sandstones occurring as isolated single-story channels (Eaton, 1991; Jinnah and Roberts, 2011). The boundary between the Reynolds Point Member and overlying Coyote Point Member is defined by Eaton (1991) as the base of a 20 m thick multi-story sandstone body, which Jinnah and Roberts (2011) describe as a gradational transition from the underlying mudstone dominated floodplain deposits of the Reynolds Point Member. The member name is derived from the Wahweap Formation lectostratotype section measured by Eaton (1991) at Reynolds Point in the Ship Mountain Point Quadrangle.

3.3. Coyote Point Member

The Coyote Point Member (formerly the upper member) comprises predominantly amalgamated tabular and lenticular sandstone deposits with a lesser proportion of fine-grained floodplain lithofacies across its 138 m thickness at Reynolds Point (Eaton, 1991; Jinnah and Roberts, 2011). Its fluvial floodplain depositional setting is inferred to have experienced some degree of marine influence near the base of the unit, possibly to the extent of estuarine development, as indicated by the presence of inclined heterolithic stratification, flaser bedding and possible brackish water invertebrate trace fossils (Jinnah and Roberts, 2011). The boundary between the Coyote Point Member and the overlying Pardner Canyon Member is marked by an undulatory erosional boundary incising into the Coyote Point Member by as much as two meters of vertical relief, and the introduction of coarser, highly amalgamated sandstone and conglomerate facies (Eaton, 1991; Jinnah and Roberts, 2011). This member is named for Coyote Point, which is located in the Lower Coyote Spring quadrangle and contains excellent exposures of this stratigraphic interval.

3.4. Pardner Canyon Member

The Pardner Canyon Member is a regionally extensive, lithologically distinctive unit that reflects an abrupt change in sedimentological character (Pollock, 1999; Lawton et al., 2003; Jinnah and Roberts, 2011). Varying in thickness across the Kaiparowits, Markagunt and Paunsaugunt plateaus to a maximum of ~140 m in the north, the Pardner Canyon Member is characterized by poorly sorted, cliff forming sandstones and conglomerates with thin, isolated mudstone lenses (Eaton, 1991; Pollock, 1999; Lawton et al., 2003; Titus et al., 2005; Jinnah and Roberts, 2011; Jinnah, 2013). As well as thickening towards the north, the Pardner Canyon Member also reportedly becomes coarser, where gravel conglomerates with clasts of chert and limestone occur more commonly in northern exposures on the Kaiparowits Plateau (Eaton, 1991; Lawton et al., 2003; Jinnah and Roberts, 2011; Lawton et al., 2014a). A dominance of planar-tabular bedforms at the base of the Pardner Canyon Member are indicative of a braided river depositional system, which grades to meander-style cross-bedded sandstones higher in the member (Eaton, 1991; Pollock, 1999; Jinnah and Roberts, 2011; Lawton et al., 2014a). Changes in sedimentological character at the base of the member, along with other evidence, such as seismites and *syn*-sedimentary faulting, reflect renewed tectonic activity in the adjacent thrust belt and potential onset of intra-basin Laramide movement during the deposition of the Pardner Canyon Member (Little, 1995; Pollock, 1999; Lawton et al., 2003; Hilbert-Wolf et al., 2009; Tindall et al., 2010; Lawton et al., 2014a). The member name originates from Pardner Canyon in the Pine Lake and Henrieville quadrangles where this portion of the Wahweap Formation was measured by Eaton (1991).

4. Materials and methods

4.1. Stratigraphy and field sampling

Previously studied exposures of the Wahweap Formation from across the Kaiparowits Plateau were revisited (e.g., Eaton, 1991; Jinnah and Roberts, 2011), and two new localities were studied in detail. These two

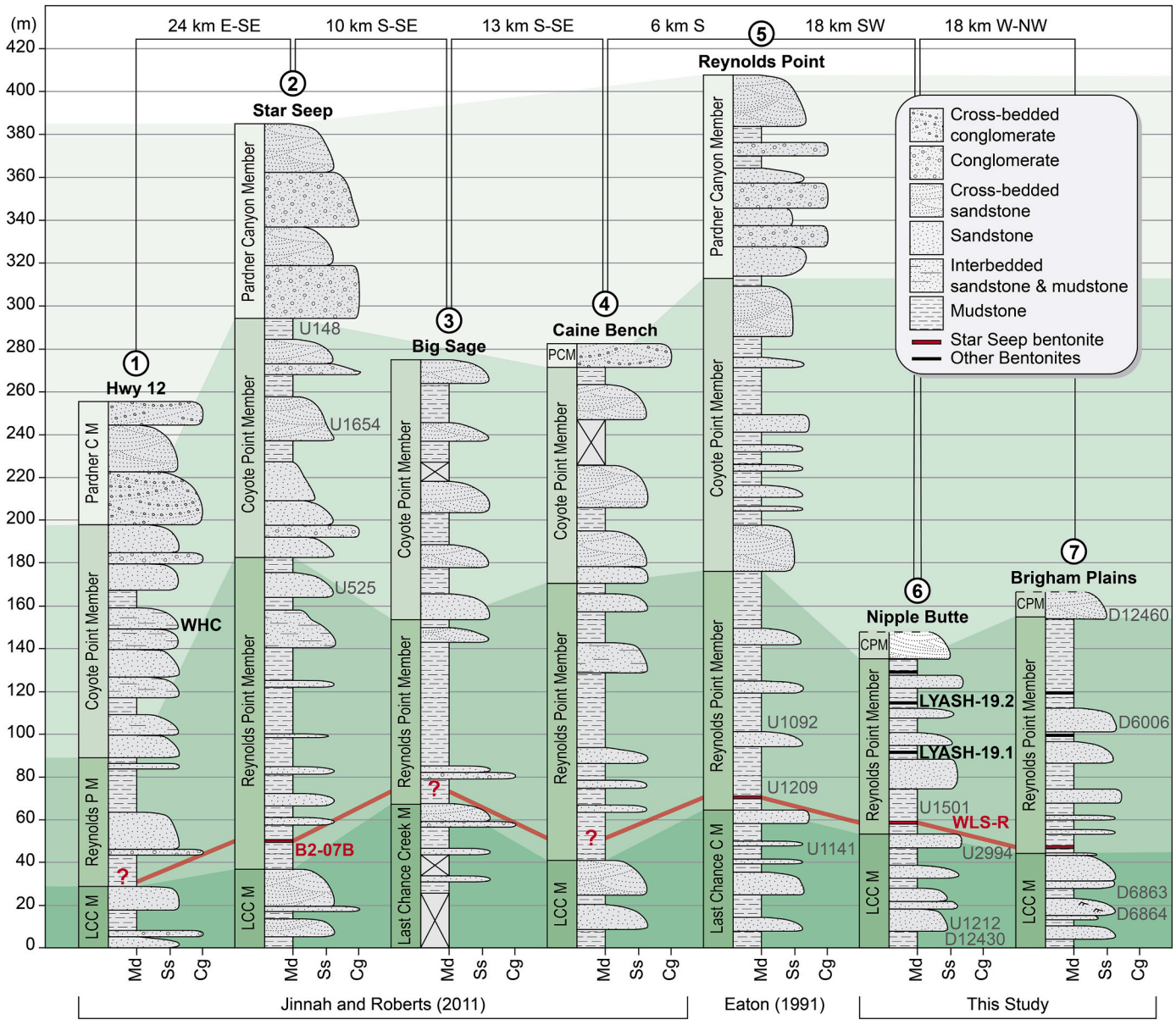

Fig. 4. Correlated stratigraphic sections of the Wahweap Formation on the Kaiparowits Plateau including sections from Eaton (1991) and Jinnah and Roberts (2011), and the most fossiliferous interval of two new localities from the southern flank of the plateau measured herein. Locality ID abbreviations: D = DMNH Loc., U = UMNH VP Loc.; see Table 3 for details about fossil localities.

localities, Nipple Butte and Brigham Plains, are located on the southern flank of the Kaiparowits Plateau (Figs. 1, 3). These sites were selected for further investigation due to excellent exposures of the Wahweap Formation, proximity to important new vertebrate fossil sites, and the presence of bentonite horizons suitable for U-Pb dating and correlation. Investigation of these sites included decimeter-scale stratigraphic sections of the most fossiliferous intervals (Fig. 4) measured using a Jacob staff and clinometer, and collection of bentonite and sandstone samples. Sandstone samples for detrital zircon analysis were also collected from the cliffs adjacent to Highway 12 at Henrieville Canyon and along Wahweap Creek at Horse Flats. An additional bentonite sample was collected from near the base of the Reynolds Point Member at Star Seep.

In situ vertebrate fossil sites cataloged by the Bureau of Land Management, Denver Museum of Nature and Science (DMNH), and Natural History Museum of Utah (UMNH) were documented using precise GPS coordinates (on file at their respective institution) and, where possible, correlated in the field to the nearest measured stratigraphic section. Other sites were plotted in Google Earth and attributed to either the lower, middle or upper portion of the lithostratigraphic members based on marker horizons (e.g., bentonites, member boundaries) visible in Google Earth satellite imagery. Localities were also categorized based on their spatial distribution across the Kaiparowits Plateau and distance from the nearest vehicle access. Field areas across the Kaiparowits Plateau were grouped as follows: South-west = Brigham Plains, Coyote Canyon, Coyote Point; South-central = Nipple Butte, Tibbet Springs, Clints Cove; South-east = Clinton Canyon, Wesses Canyon, Wesses Cove, Ship Mountain Point, Pilots Knoll; Central = The Gut; North = Right Hand Collet Canyon, Star Seep, Camp Flat, Death Ridge (see Fig. 1). Distance from the nearest vehicle access was measured in Google Earth as direct map distance and results were characterized as: close = 0–249 m; moderately close = 250–499 m; moderately far = 500–749 m; far = 750–999 m; distal ≥1000 m.

4.2. U-Pb LA-ICP-MS geochronology of sandstones

Detrital zircons were separated from five sandstone samples by

standard mineral separation methods, including random-grain representative selection of all morphologies, and analyzed for U and Pb isotopes by LA-ICP-MS at the Advanced Analytical Centre at James Cook University as outlined in Beveridge et al. (2020). A Teledyne Analyte G2193 nm Excimer Laser with HeLex II Sample Cell was used to ablate 25 μm pits in the zircons and liberated material was analyzed in a Thermo iCAP-RQ ICP-MS (see Todd et al., 2019 and Huang et al., 2021 for further details on laboratory procedures). Zircon mineral standards used included GJ1 (primary), and Plesovice and 91500 (secondary). All uranium-lead LA-ICP-MS data were reduced in the Iolite software package (iolite-software.com) and weighted mean ages were calculated using Isoplot (Ludwig, 2012). Complete data are given in Supplementary material 2. Individual zircon grain ages with >5% discordance or > 5% 2σ propagated uncertainty (Y) were discarded. Maximum estimates of depositional ages were calculated, where appropriate, based on weighted mean $^{206}Pb/^{238}U$ dates of the youngest population of overlapping analyses, and reported at a 95% confidence interval in the format ± X/Y Ma, where X includes the internal uncertainty only and Y incorporates a calculated estimate of external reproducibility. Results are summarized in Table 1 and Figs. 5 and 6.

4.3. U-Pb CA-ID-TIMS geochronology of ash fall bentonites

High-precision U-Pb zircon analyses by the CA-ID-TIMS technique were conducted at the Massachusetts Institute of Technology Isotope Laboratory using procedures described in Ramezani et al. (2011). Bulk bentonite samples were processed in a sonic dismembrator device (Hoke et al., 2014) designed to break apart and remove the clay component before heavy mineral separation by standard magnetic and high-density liquid separation techniques. The target zircon population of the two ash fall bentonites was selected under a binocular microscope according to a set of morphological criteria including faceted prismatic habit, high aspect ratio (1:5) and presence of elongated glass (melt) inclusions parallel to the crystallographic "C" axis. This selection approach has proven effective in screening reworked zircons (Ramezani et al., 2011). Selected grains were pretreated by a chemical abrasion technique modified after Mattinson (2005), which involved thermal annealing at 900 °C for 60 h before partial dissolution in 28 M hydrofluoric acid at 210 °C in a high-pressure digestion vessel for 12 h. After thorough fluxing and rinsing to remove the leachates, the zircons were spiked with the EARTHTIME ET2535 mixed U-Pb tracer solution (McLean et al., 2011, 2015; Condon et al., 2015) and completely dissolved in 28 M HF at 210 °C for 48 h. Chemically purified Pb and U via anion-exchange column chemistry were subsequently analyzed on an Isotopx X62 thermal ionization mass spectrometer with nine Faraday detectors and a Daly ion counting system. Data reduction and error propagation were conducted using Tripoli and ET_Redux software (Bowring et al., 2011; McLean et al., 2011). Complete data are given in Supplementary material 2. Bentonite ages are derived from the weighted mean $^{206}Pb/^{238}U$ dates of the analyzed zircons after excluding visibly older analyses interpreted as xenocrystic or detrital; no zircon analyses from the young end of the age spectra were excluded from the weighted mean. Calculated age uncertainties are reported in the ± X/Y/Z format, where X is the internal 95% confidence interval uncertainty in the absence of all external errors, Y incorporates X and the tracer calibration errors, and Z includes Y as well as the U decay constant uncertainties of Jaffey et al. (1971). Results are summarized in Table 1 and Fig. 5.

4.4. U-Pb LA-ICP-MS geochronology of reworked bentonites

Three additional bentonite samples from the Reynolds Point Member of the Wahweap Formation at Nipple Butte were also examined; however, each sample appeared to contain varying degrees of visibly detrital material, which suggested the horizons may have been partly reworked. Due to the increased likelihood of detrital incorporation, a mixed approach to dating these bentonites was employed. Zircon grains from these samples were selected using the same morphological criteria as for ash fall bentonites; however, the resulting grains were analyzed using the LA-ICP-MS approach and treated as maximum depositional ages. Complete data are given in Supplementary material 2 and summarized in Table 1 and Fig. 5.

4.5. Comparison of U-Pb data

Within this study, and when comparing data from this study with others, consideration must be made with respect to the choice of uncertainties if meaningful comparisons are to be made between radioisotopic dates that resulted from different chronometers or produced by different techniques. In comparing U-Pb dates from different techniques (i.e., LA-ICP-MS versus CA-ID-TIMS), the Y uncertainty should be used, whereas for comparing U-Pb and $^{40}Ar/^{39}Ar$ dates, it is necessary to include decay constant uncertainties (Z). Previous investigations have also shown that mean ages from the same zircon crystals generated using CA-ID-TIMS and microbeam techniques (i.e., LA-ICP-MS, and secondary ion mass spectrometry [SIMS]) may not always overlap within stated uncertainties (von Quadt et al., 2014; Ickert et al., 2015; Herriott et al., 2019; Rasmussen et al., 2021). Various factors are implicated in this possible bias (e.g., untreated Pb loss, difficulty defining youngest population thresholds, use of mineral standards) and discrepancies in mean ages are not exclusively younger or older (e.g., Herriott et al., 2019; Rasmussen et al., 2021); thus, it is possible that the LA-ICP-MS ages reported in our study have additional geologic uncertainty not encapsulated by the reported internal (X) or propagated (Y) uncertainties. As well as being treated as MDAs due to the potential incorporation of detrital material in samples chosen for LA-ICP-MS analysis in this study, we recommend that these ages are used mindfully when comparing with ages generated using different techniques and/or chronometers.

4.6. Bayesian age model

A quantitative chronostratigraphic model was constructed for the Wahweap Formation based on our dated horizons and their stratigraphic positions to calculate robust ages and uncertainty for any stratigraphic horizon of interest (e.g., fossil localities, member boundaries). This was accomplished using the Compound Poisson-Gamma Bayesian statistical approach of Haslett and Parnell (2008) with a modified Markov chain Monte Carlo fitting algorithm included in the Bchronology R software package (Parnell et al., 2008, 2011). By considering variable sediment accumulation rates using Poisson random variability, the Bchron statistical approach more appropriately propagates stratigraphic uncertainty (Haslett and Parnell, 2008; Parnell et al., 2008, 2011; De Vleeschouwer and Parnell, 2014; Trayler et al., 2020) compared to simple linear extrapolation, which assumes a constant sedimentation rate and thus falls short of realistic error propagation leading to over-optimistic uncertainty (De Vleeschouwer and Parnell, 2014). The Bayesian age-stratigraphic model is illustrated with a median (black line, Fig. 7), somewhat comparable to a linear model, and a 95% uncertainty envelope (blue shaded area, Fig. 7), which tends to balloon (i.e., elevated stratigraphic age uncertainty) with distance from dated horizons.

The chronostratigraphic data produced in our study were modeled alongside the Reynolds Point lectostratotype section of Eaton (1991) and the Y uncertainties for both CA-ID-TIMS and LA-ICP-MS dates were used in the model construction. The graphical output of the model, shown in Fig. 7, provides a useful tool for visualizing age-stratigraphic uncertainty, while the numerical output (Supplementary material 3) lists a series of model ages represented by the median of predicted values and their 95% confidence level asymmetric uncertainties. All calculations were conducted in R Studio and relevant information including scripts can be found in Supplementary material 3.

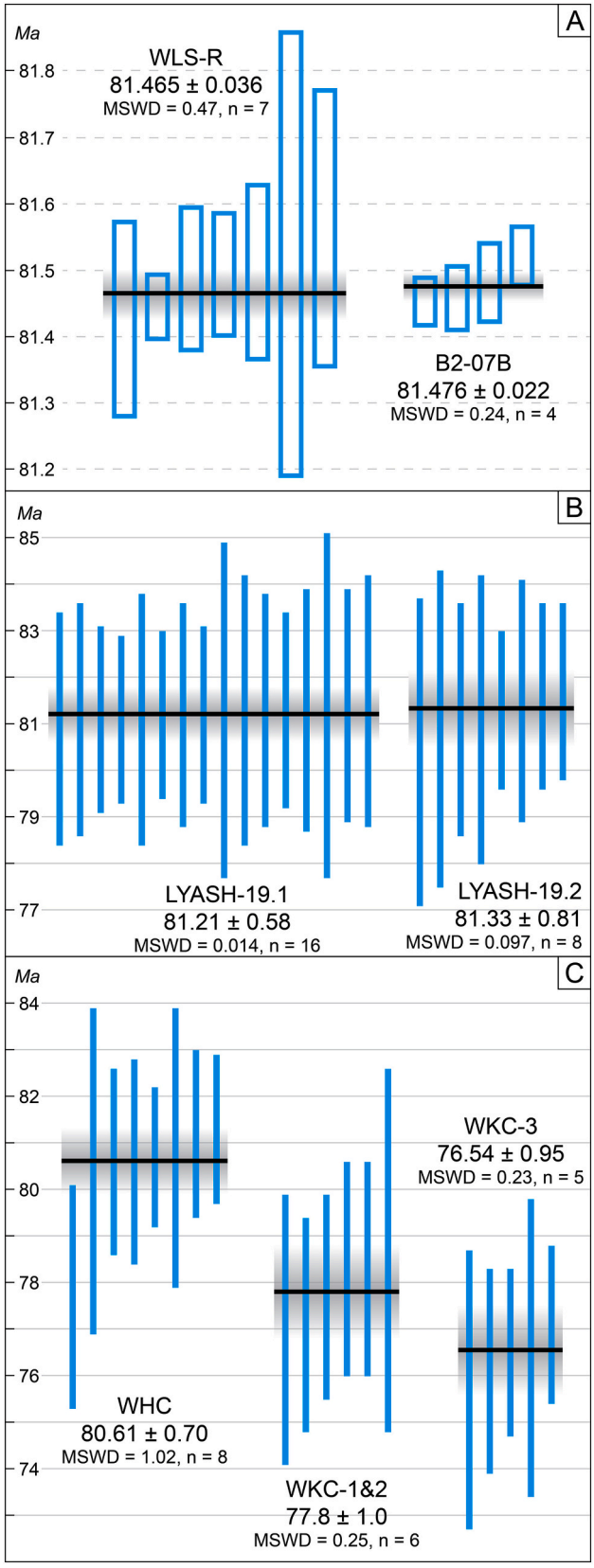

Fig. 5. Plots of zircon $^{206}Pb/^{238}U$ dates with 2σ uncertainties (vertical bars) and their calculated weighted mean (horizontal bar) with a 95% error envelope (shaded band) for each sample. A) CA-ID-TIMS pure bentonite ages. B) LA-ICP-MS reworked bentonite ages. C) LA-ICP-MS detrital zircon maximum depositional ages.

5. Geochronological results

5.1. Results: High-precision CA-ID-TIMS bentonite ages

We report two high-precision U-Pb ages for the Wahweap Formation (Table 1, Fig. 5). The first sample (B2-07B) was collected from the same horizon as the previously dated $^{40}Ar/^{39}Ar$ sample SS07-B (Jinnah, 2013) at Star Seep, 54 m above the base of the formation (Fig. 4). This bentonite, which is also presumably correlative with (or within ±5 m of) bentonite CF05-B from Jinnah et al. (2009), is located near the base of the Reynolds Point Member ~10 m above a distinctive, laterally continuous sandstone that marks the top of the Last Chance Creek Member. The bentonite horizon is ca 20 cm thick, and the weathered outcrop shows characteristic popcorn swelling textures. Unweathered rock is yellowish-green in color with visible black flecks (biotite phenocrysts) and minimal translucent grains (e.g., quartz). Our new dating yielded a weighted mean $^{206}Pb/^{238}U$ age of 81.476 ± 0.022/0.031/0.092 Ma (2σ) (MSWD = 2.2) based on four youngest overlapping zircon analyses. Besides a more than twenty-fold improvement in precision, this new age is 1.6 ± 0.6 million years older than the previous $^{40}Ar/^{39}Ar$ age of 79.9 ± 0.6 Ma for the same bed, which is outside its reported (2σ internal) uncertainty (see Fig. 7). Similarly, it is 0.9 ± 0.6 million years older than that of the correlative (or within ±5 m) CF05-B bentonite (80.6 ± 0.6 Ma) (Jinnah et al., 2009; Jinnah, 2013).

The second bentonite sample (WLS-R) was collected from Nipple Butte on the southern flank of the Kaiparowits Plateau and represents the first dated bentonite from the entire southern extent of the formation. The bentonite horizon is located 60 m above the base of the Wahweap Formation at Nipple Butte and, much like B2-07B from the northern field area, the WLS-R sample was collected ~5 m above a distinctive, laterally continuous cross-bedded sandstone that marks the top of the Last Chance Creek Member. Characteristic swelling textures were also observed at this locality, and the ca 25 cm thick pistachio green horizon of unweathered material also exhibited visible black flecks and had a waxy smectite texture. This sample yielded a weighted mean $^{206}Pb/^{238}U$ age of 81.465 ± 0.036/0.042/0.097 Ma (2σ) (MSWD = 0.47) based on all of its seven zircon analyses with no outliers.

Both high-precision CA-ID-TIMS bentonite ages are within analytical (X) uncertainty of each other, which supports our field-based assessment that they represent the same bentonite horizon outcropping approximately ~38 km apart. We refer to this widespread bentonite marker horizon as the Star Seep bentonite after the locality from which it was initially studied (Jinnah et al., 2009; Jinnah, 2013) and it serves as a reliable tie point for correlating the Wahweap Formation across the Kaiparowits Plateau (e.g., Fig. 4).

5.2. Results: Reworked bentonite LA-ICP-MS ages

Alongside high-precision CA-ID-TIMS geochronology for ash fall bentonites from the Wahweap Formation, this study also reports supporting $^{206}Pb/^{238}U$ LA-ICP-MS ages for suspected reworked bentonite horizons that are interpreted as maximum depositional ages. Three such bentonite horizons were identified in the Reynolds Point Member of the Wahweap Formation at Nipple Butte and can also be observed in other stratigraphic sections (e.g., Brigham Plains, Fig. 4). Samples were collected from 117 m (LYASH-19.1), 148 m (LYASH-19.2) and 163 m (LYASH-19.3) above the base of the formation at Nipple Butte.

Despite showing mineralogical evidence of some degree of detrital material, two of these three bentonite samples produced statistically coherent age populations within the uncertainties of the LA-ICP-MS analyses (Table 1, Fig. 5). The stratigraphically lowest reworked bentonite, LYASH-19.1, yielded a weighted mean age of 81.21 ± 0.53/0.58 Ma (2σ) (MSWD = 0.014) from a young population of 16 zircons. Based on crystal morphology and distribution of zircon ages, this bentonite age is considered a close approximation of the true depositional age. LYASH-19.2, which is 23 m stratigraphically higher than the

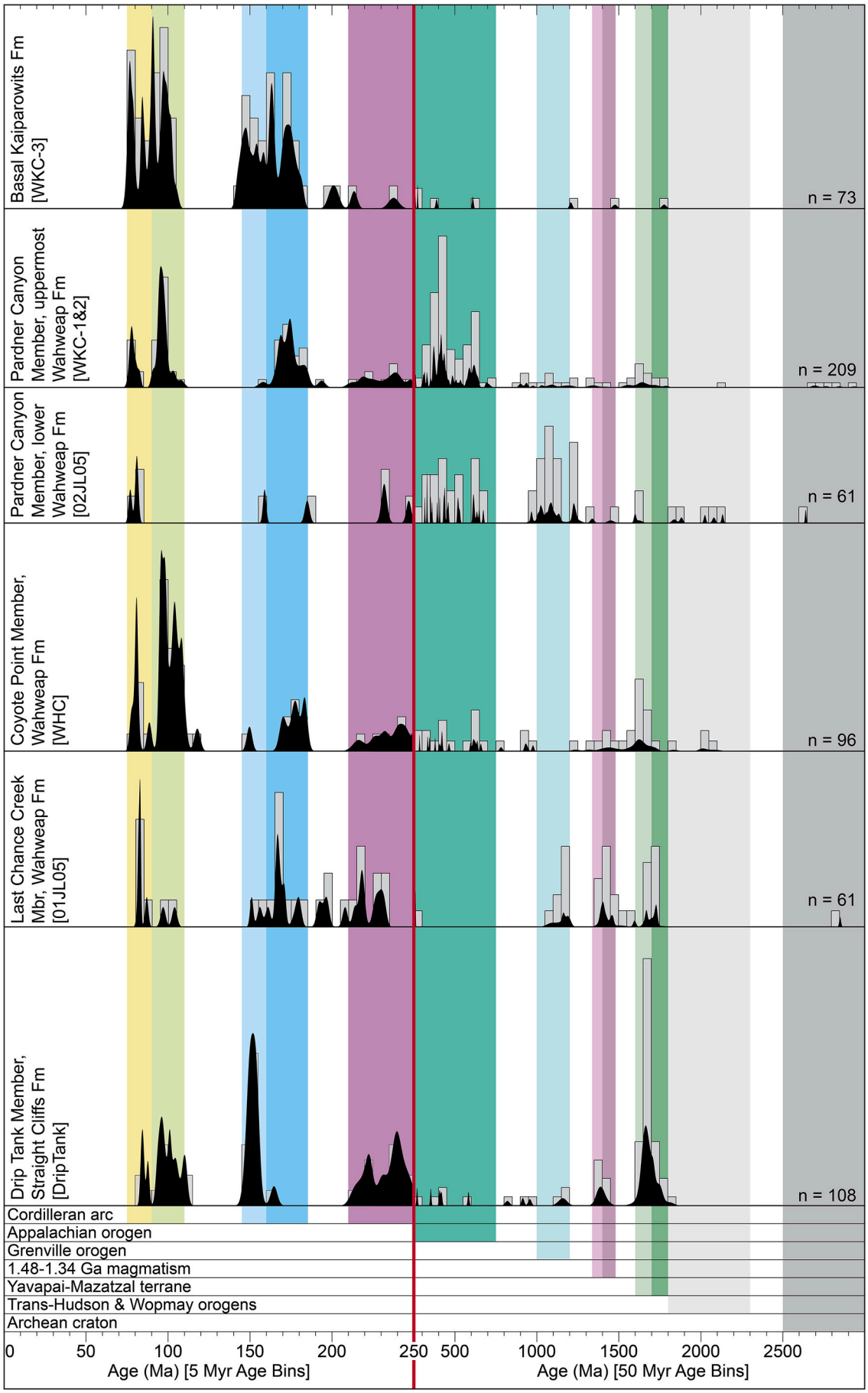

(caption on next page)

Fig. 6. Probability distribution plots of detrital zircon U-Pb dates including samples 01JL05 and 02JL05 from Jinnah et al. (2009). Note the change in x-axis scale at the Permian-Triassic boundary, applied here to highlight significant discrepancies in Mesozoic zircon groups. Y-axis is scaled proportionally based on grain age frequency and number of grains per sample to facilitate direct comparison of modes and groups. Age groupings adapted from Laskowski et al. (2013) and references therein.

previous sample, produced a weighted mean age of 81.33 ± 0.72/0.81 Ma (2σ) (MSWD = 0.097) from a young population of eight grains. Compared to the stratigraphically lower LYASH-19.1 and the CA-ID-TIMS dated Star Seep bentonite, the LYASH-19.2 results appear older than the expected age, probably due to incorporation of reworked zircons. The bentonite that showed the greatest degree of reworking (LYASH-19.3), did not yield a young coherent age population and therefore no depositional age can be calculated.

5.3. Results: Detrital zircon LA-ICP-MS ages

Additional age constraints for the Wahweap Formation were attained using five sandstone detrital zircon (DZ) samples from the Wahweap Formation, the underlying Straight Cliffs Formation, and the overlying Kaiparowits Formation. Maximum depositional ages (MDAs) for DZ samples were calculated using the weighted mean age of the youngest coherent population (YCP) (Table 1, Fig. 5). Sample "DripTank" from immediately below the Wahweap Formation at the top of the Drip Tank Member of the Straight Cliffs Formation did not yield a coherent young population, but the youngest single grain age was 83.8 ± 1.4/1.7 Ma. A DZ sample was collected from cliffs adjacent to Highway 12 along Henrieville Canyon in the middle of the Coyote Point Member of the Wahweap Formation (~150 m above the base of the formation at this location, Fig. 4). This sample produced a MDA of 80.61 ± 0.69/0.70 Ma (MSWD = 1.02) from a YCP of eight zircons. Three detrital zircon samples that bracket the top of the Wahweap Formation were collected across a distinctive pedogenic surface inferred to be the top boundary of the Wahweap Formation at Horse Flats (Fig. 8). WKC-1 and WKC-2 consist of fine (to muddy) and medium grain quartz-arenite sandstones (respectively) from immediately below the pedogenic surface. Based on proximity and lithological similarity, these two samples were grouped together and this DZ suite produced a MDA of 77.8 ± 0.93/1.0 Ma (MSWD = 0.25) calculated from a YCP of six grains. WKC-3, collected from a lithic arkose immediately above the pedogenic surface at the very base of the Kaiparowits Formation, yielded a MDA of 76.54 ± 0.87/0.95 Ma (MSWD = 0.23) from five grains. Overall, the MDAs exhibit good correlation between their stratigraphic position and true depositional ages from bracketing ash fall bentonites, which we infer makes them reasonable approximations of the depositional age.

The provenance of sandstones from the Wahweap Formation has been examined previously in great detail (e.g., Dickinson and Gehrels, 2008; Larsen et al., 2010; Dickinson et al., 2012; Lawton and Bradford, 2011; Lawton et al., 2014b), and was not the focus of this investigation; however, broad observations are reported here based on detrital zircon age spectra illustrated in Fig. 6. For comparison, Fig. 6 also includes two previous detrital zircon samples (01JL05, 02JL05) described by Jinnah et al. (2009). The four new samples highlight important trends in provenance, particularly across unconformities and formation boundaries (see Fig. 6). The single Drip Tank Member sample from immediately below the Wahweap Formation contains a notable mode at 151 Ma, a substantial Triassic cluster (14%), and major groups at ca 1.4 Ga and 1.7 Ga, the latter of which comprises 42% of the total grain count. Sample WHC from the Coyote Point Member of the Wahweap Formation is dominated by Cretaceous grain ages representing 39% of the total suite along with a broad group around 179 Ma and minor Paleozoic and Proterozoic groupings. Samples WKC-1&2 from the top of the Wahweap Formation in the Pardner Canyon Member contain Mesozoic groups with modes at 79 Ma, 96 Ma, 171 Ma and a minor suite of Triassic grains, as well as a major group of Paleozoic ages (36%). Sample WKC-3 from the base of the Kaiparowits Formation is best described as two dominant multi-modal groups; one from the Late Cretaceous and the other from the Middle to Late Jurassic. Interestingly, this sample contains only a handful of grains older than 200 Ma (<14%).

6. A new chronostratigraphic framework for the Wahweap Formation

Two new high-precision CA-ID-TIMS and five supporting LA-ICP-MS U-Pb zircon ages from a variety of stratigraphically well-constrained bentonites and sandstones form the basis of a new age model for the Wahweap Formation generated using a Bayesian statistical method. We find that the age of the Wahweap Formation ranges from approximately 82.17 +1.5/-0.63 Ma to 77.29 +0.72/-0.62 Ma, coinciding with the first half of the Campanian Stage (Table 2, Fig. 7). The new

Table 1
Weighted mean U-Pb zircon ages for all samples analyzed in this study (in stratigraphic order) including bentonite true ages and detrital zircon and bentonite maximum depositional ages. Additional data are not included here due to limited equivalency between CA-ID-TIMS and LA-ICP-MS datasets. Complete data are included in Supplementary Material 2.

Method / Age Type	Sample Name	Outcrop Area	Lithostratigraphic Member	Stratigraphic Height* (m)	Weighted Mean Age					
					$^{206}Pb/^{238}U$ Age (Ma)	Error (2σ)^			MSWD	n#
						X	Y	Z		
Detrital Zircon LA-ICP-MS / Maximum Depositional Age	WKC-3	Horse Flat	lower Kaiparowits Fm	415	76.54	0.87	0.95	–	0.23	5
	WKC-1 & 2	Horse Flat	Pardner Canyon Member	405	77.8	0.93	1.0	–	0.25	6
	WHC	Hw12	Coyote Point Member	245	80.61	0.69	0.70	–	1.02	8
Bentonite LA-ICP-MS / Maximum Depositional Age	LYASH-19.2	Nipple Butte	Reynolds Point Member	148	81.33	0.72	0.81	–	0.097	8
	LYASH-19.1	Nipple Butte	Reynolds Point Member	117	81.21	0.53	0.58	–	0.014	16
Bentonite CA-ID-TIMS / True Depositional Age	WLS-R	Nipple Butte	Reynolds Point Member	72	81.465	0.036	0.042	0.097	0.47	7
	B2-07B	Star Seep	Reynolds Point Member	72	81.476	0.022	0.031	0.092	2.20	4

MSWD = mean square of weighted deviates. n# = number of analyses included in the calculated weighted mean age.
* Meters above the base of the Wahweap Formation relative to Reynolds Point lectostratotype section of Eaton (1991).
^ Error for CA-ID-TIMS (X = analytical uncertainty in the absence of all external or systematic errors, Y = X plus U-Pb tracer calibration error, Z = Y plus U decay constant uncertainties) and LA-ICP-MS (X = internal uncertainty, Y = propagated uncertainty).

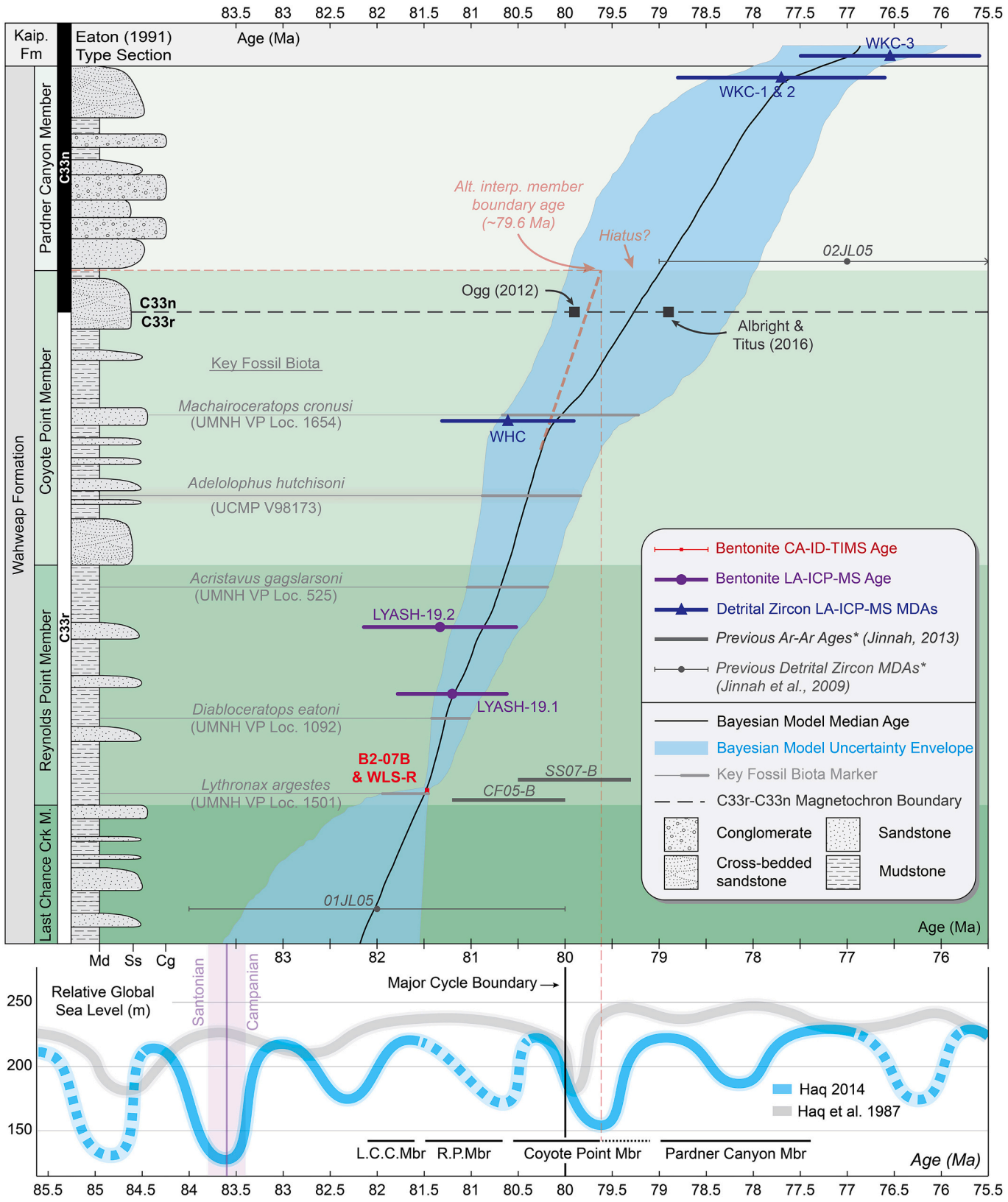

Fig. 7. U-Pb geochronology and Bayesian age-stratigraphic model for the Wahweap Formation against the Reynolds Point lectostratotype section of Eaton (1991) with global sea level curves (Haq et al., 1987; Haq, 2014) (NB: thickness of sea level curves does not reflect data precision). Due to lateral variation in unit thickness of the Wahweap Formation on the Kaiparowits Plateau, absolute stratigraphic height is not shown. Rock and vertebrate fossil specimens were stratigraphically correlated from their nearest measured section to the Reynolds Point lectostratotype section. Red dashed lines illustrate an alternate interpretation of the age of the Coyote Point – Pardner Canyon member boundary. * Ages that were not used in the generation of the Bayesian model. (For interpretation of the references to color in this figure legend, the reader is referred to the web version of this article.)

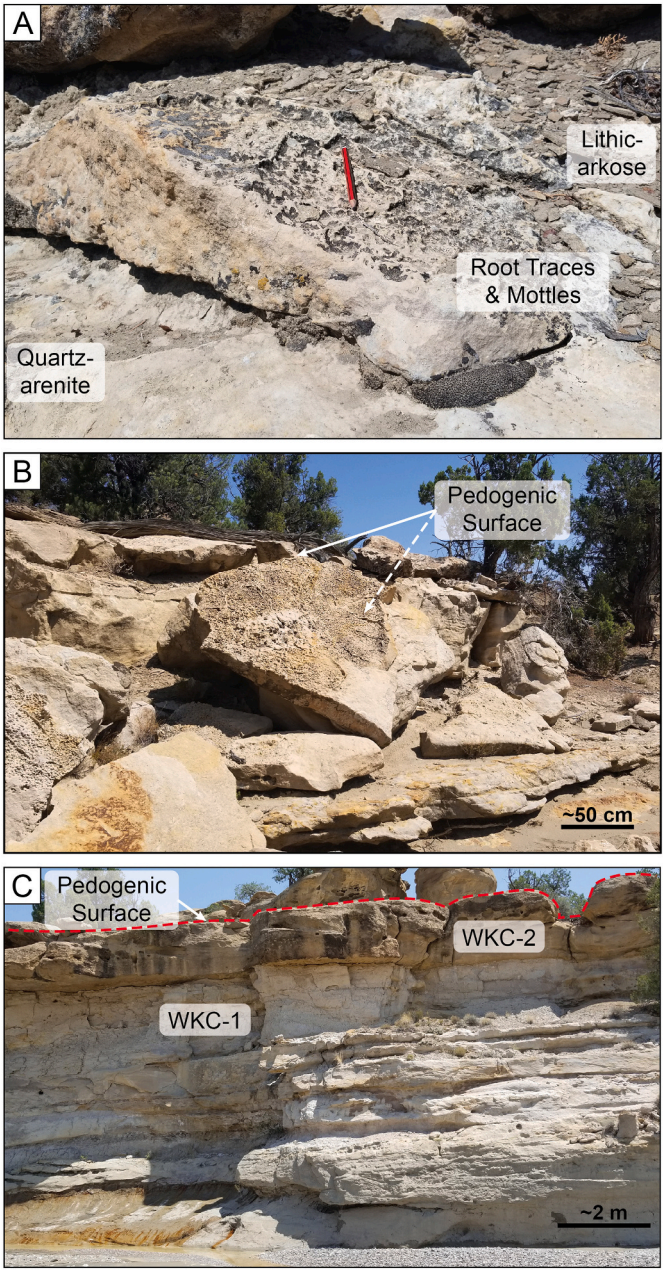

Fig. 8. Annotated photographs of the pedogenic surface that separates the Wahweap and Kaiparowits formations at Horse Flat (see Fig. 1). A) Close-up showing a mottled surface with root traces separating Kaiparowits lithic arkose and Wahweap quartz arenite sandstones (pencil for scale). B) Displaced block of uppermost Wahweap Formation sandstone showing the texture of the boundary with the Kaiparowits Formation. C) Exposure illustrating sampled lithologies (WKC-3 collected above the dashed line) where the muddy, fine grained sandstone WKC-1 would previously have been designated as the formation boundary.

chronostratigraphic model indicates the base of the formation is ca 1.2 million years older than previous estimates (i.e., Jinnah et al., 2009; Jinnah, 2013) and provides objective age constraints on Wahweap fossil biota. The revised basal age confirms that the formation does indeed cover an interval of the early Campanian (e.g., Eaton, 1991), contrary to the previous interpretation by Jinnah et al. (2009). Temporal extension of the Wahweap Formation means that strata of the combined Wahweap and overlying Kaiparowits formations (including the recently described Upper Valley Member of the Kaiparowits Formation; see Beveridge et al., 2020), with a combined thickness of approx. 1.4 km, encompass nearly the entire Campanian stage.

Table 2
Model ages for member boundaries generated using the Bayesian age-stratigraphic model (Fig. 7, Supplementary Material 3). Note the asymmetrical uncertainty, which is related to the model's 95% confidence window.

Stratigraphic Level of Interest	Stratigraphic Height* (m)	Model Age (Ma)	2σ Uncertainty	
			+	−
Top of Wahweap Fm	410	77.29	0.72	0.62
Coyote Point – Pardner Canyon Mbr Boundary	313	79.00	0.98	0.99
Reynolds Point – Coyote Point Mbr Boundary	176	80.61	0.39	0.51
Last Chance Creek – Reynolds Point Mbr Boundary	65	81.55	0.62	0.09
Base of Wahweap Fm	0	82.17	1.47	0.63

* Relative to Reynolds Point lectostratotype section of Eaton (1991).

6.1. Member boundaries and features

Model boundary ages of the newly formalized subdivisions of the Wahweap Formation reported in Table 2 are based on stratigraphic thicknesses at the lectostratotype section of Eaton (1991) measured at Reynolds Point in the Ship Mountain Point Quadrangle (Fig. 7). Member boundaries in the Wahweap Formation are generally considered isochronous across the Kaiparowits Plateau because the mechanisms that govern the alluvial architecture which defines the members are believed to act near synchronously across the immediate area (Jinnah and Roberts, 2011; Jinnah, 2013). The lower two boundaries appear to be simple and conformable; however, sedimentologic evidence indicates a significant depositional hiatus between the Coyote Point and Pardner Canyon members (Eaton, 1991; Jinnah and Roberts, 2011; this study); thus, the time interval represented by this boundary requires closer examination. Our Bayesian age model yields a member boundary age of 79.0 Ma with a large uncertainty window of approximately two million years resulting from sparsity and imprecision of constraining ages in this portion of the stratigraphy. The presence of a depositional hiatus in this broadly constrained section undoubtedly impacts the accuracy of the model age; although, the comparatively large uncertainty accommodates various interpretations for the age of the member boundary. For example, linear extrapolation of the sediment accumulation rate from the well-constrained Reynolds Point Member (~13 cm/ka) suggests an older boundary age closer to ~79.6 Ma, which still falls within the error window of the chronostratigraphic model (see Fig. 7). This alternate interpretation has implications for sequence stratigraphic models of the Wahweap Formation as it aligns the depositional hiatus at the top of the Coyote Point Member with a global sea level minimum (i.e., major sequence boundary; see Haq, 2014). Our chronostratigraphic model further supports sequence stratigraphic interpretations discussed by Jinnah and Roberts (2011; and references within), although with slightly revised chronological constraint. Jinnah and Roberts (2011) discuss evidence of marine incursion close to the base of the Coyote Point Member, which our model indicates is coincident with the preceding eustatic sea level maximum (Fig. 7). Future work may be able to revisit this interpretation using additional age constrains from the Coyote Point and Pardner Canyon members.

As well as implications for sequence stratigraphy, the age of the upper Coyote Point Member, including the alternate interpretation discussed above, is relevant to the C33r-C33n polarity reversal boundary identified by Albright and Titus (2016) at ~270 m above the base of the Wahweap Formation. The C33r-C33n boundary was previously interpreted to occur at 79.9 Ma (GST2012 – Ogg, 2012) based on two $^{40}Ar/^{39}Ar$ bentonite ages and linear extrapolation in the Elk Basin; however, Albright and Titus (2016) recalculated these $^{40}Ar/^{39}Ar$ ages and report a revised magnetochron boundary age of 78.91 Ma.

Interestingly, our model age at 270 m above the base of the Wahweap Formation (79.30 +1.05/-0.83 Ma at 293 m in the Reynolds Point lectostratotype section) is marginally closer to the Albright and Titus (2016) revised magnetochron boundary age, while the alternate interpretation discussed above aligns more closely with previous interpretations of the boundary age (i.e., GTS2012 – Ogg, 2012). Most importantly, both interpretations for the age of the C33r-C33n polarity reversal boundary fall within the uncertainty envelope of our model and, given the uncertainty associated with the $^{40}Ar/^{39}Ar$ ages from the Elk Basin that constrain the chron boundary, the two suggested ages are also probably within error of each other. Further investigation thus requires additional age constraints from the upper two members of the Wahweap Formation, which may lead to more definitive age assignment of the C33r-C33n polarity reversal boundary.

6.2. Upper and basal formation boundaries

The age of the upper boundary of the Wahweap Formation, 77.29 +0.72/-0.62 Ma, matches closely with previous estimates and, furthermore, the detrital zircon U-Pb data in our study provide useful insights into the nature of the contact. The upper boundary of the Wahweap Formation has been described in previous studies to be variously erosional and/or conformable with little clear consensus (Peterson, 1969; Eaton, 1991; Little, 1995; Pollock, 1999; Roberts, 2007; Jinnah and Roberts, 2011; Lawton et al., 2014a). The most consistent description states that the contact is erosional across much of the Kaiparowits Plateau but locally gradational where continuous sections were measured (Jinnah and Roberts, 2011), which we interpret to be proximal to The Blues adjacent to Highway 12 and Henrieville Creek (Fig. 1). This description matches our field observations closely. A pedogenic erosional surface with root traces and mottling observed in our study at Horse Flat (Fig. 8) likely represents only a short hiatus, as indicated by the overlapping detrital zircon MDAs from the either side (± 5 m) of the pedogenic surface (Fig. 5), although the large uncertainties of these MDAs preclude the exact quantification of this hiatus. Conversely, an immediate shift in sedimentology and provenance across the surface is reflected by the sudden appearance of significant proportions of chert lithics and a large Late Jurassic zircon age group, as illustrated in Figs. 6 and 8. Observation of an erosional surface separating visibly dissimilar sandstones (quartz arenite versus lithic arkose) that have distinct detrital zircon age spectra, supported by the inference that the duration of hiatus was minimal, suggests an abrupt change in sediment source, which marks the transition between the Wahweap and Kaiparowits formations. This interpretation also explains reports of a transitional zone of interfingering sandstones of varying provenance described elsewhere in the study area (Jinnah and Roberts, 2011; Lawton et al., 2014a). As well as at the upper boundary of the Wahweap Formation, an abrupt change in sediment source is also noted across the unconformity at the Coyote Point – Pardner Canyon member boundary, evident most clearly by the sudden scarcity of Mesozoic grains when comparing data from this study and that of Jinnah et al. (2009)(Fig. 6).

Unlike that of the upper boundary, the age of the base of the Wahweap Formation demands a significant revision due to new chronostratigraphic data reported here. Previous estimates using $^{40}Ar/^{39}Ar$ absolute ages and linear sediment accumulation rates estimated the base of the formation to occur at ~81 Ma (Jinnah, 2013). The new high-precision $^{206}Pb/^{238}U$ CA-ID-TIMS age of ~81.47 Ma for the Star Seep bentonite (a combination of the overlapping B2-07B age of 81.476 ± 0.031[Y] Ma and the WLS-R age of 81.465 ± 0.042[Y] Ma), is significantly older (~0.9 to 1.6 Myr) than previous ages for what is interpreted to be the same horizon (SS07-B = 79.9 Ma, CF05-B = 80.6 Ma – Jinnah et al., 2009; Jinnah, 2013). The new Bayesian model age for base of the Wahweap Formation is 82.17 +1.47/-0.63 Ma, which agrees well with detrital zircon MDAs from Jinnah et al. (2009) and with magnetostratigraphic data from Albright and Titus (2016); however, it is older than the MDA reported by Szwarc et al. (2015) for the underlying Drip Tank Member of the Straight Cliff Formation. Conversely, reinterpretation of the dataset from Szwarc et al. (2015) by removing single grain ages younger than the Star Seep bentonite age presented here yields a revised MDA for the Drip Tank Member of 83.49 ± 0.62 Ma from five grains, which matches more closely with findings from our study and others (e.g., Jinnah et al., 2009; Albright and Titus, 2016) although further chronologic work on the Drip Tank Member is recommended.

6.3. Regional correlation

Our revision of the age of the Wahweap Formation has significant implications for correlative units across the Western Interior. Current age estimates for presumed coeval units in the nearby Henry Basin, east of the Kaiparowits Plateau (Fig. 2), are based on constraints from the Wahweap Formation (Eaton, 1990; Corbett et al., 2011; Seymour and Fielding, 2013; Lawton et al., 2014a). Corresponding strata of the Henry Basin record coastal floodplain depositional environments, including the Masuk Formation and the Tarantula Mesa Sandstone which are believed to be equivalent to the Wahweap Formation's Last Chance Creek, Reynolds Point and Coyote Point members and the Pardner Canyon Member, respectively (Eaton, 1990; Corbett et al., 2011). Assuming these units are indeed contemporaneous, the updated geochronology reported in this study also revises the chronology of the Henry Basin strata, as illustrated in Fig. 9. Substantiating more formal correlation of the Kaiparowits Plateau and Henry Basin strata across the extensive gap in exposure between these areas would require future detailed lithostratigraphic work including adjustments to the unit hierarchy and, as such, is not considered further herein.

At a broader geographic scale, adjustments to the age of the Wahweap Formation also have implications for correlation across the Western Interior (Figs. 2 and 9). Most significantly, we support and expand upon findings of Albright and Titus (2016) that the Last Chance Creek, Reynolds Point, and Coyote Point members are older than the richly fossiliferous Belly River Group in southern Alberta (Eberth, 2005, 2015) and Judith River Formation in central Montana (Foreman et al., 2008; Rogers et al., 2016). Campanian formations across western North America that are found to be partly or fully contemporaneous with the Wahweap Formation (including the Pardner Canyon Member) include: the Pakowki, Foremost and lower Oldman formations in southern Alberta (Payenberg et al., 2002; Eberth, 2005, 2015); the Two Medicine Formation and Claggett Shale in northwest Montana (Foreman et al., 2008; Rogers et al., 2016); the Eagle Formation and Claggett Shale, as well as the Parkman Sandstone and lower McClelland Ferry members of the Judith River Formation in central Montana (Rogers et al., 2016); the Blue Gate Shale, Blackhawk and Castlegate formations in central and eastern Utah (Seymour and Fielding, 2013); the Menefee Formation, Cliff House Sandstone and Lewis Shale in southern exposures of the San Juan Basin in northwest New Mexico (Cather, 2004; Fassett and Heizler, 2017), and the lower Aguja Formation in West Texas and northern Chihuahua/Coahuila (Lehman et al., 2019). Higher resolution geochronological constraints are needed for many of these presumed coeval units as correlation of their fossil-bearing intervals is invaluable to our collective understanding of faunal and floral diversity across Laramidia during the Late Cretaceous.

6.4. North American Land Mammal Ages

Refinement of the age and basin-scale correlation of the Wahweap Formation enables re-examination of its relationship to the Late Cretaceous North American Land Mammal Ages (NALMA). The unique mammaliaform assemblage of the Wahweap Formation has proven difficult to place into the NALMA framework, with previous studies suggesting either Aquilan or Judithian affinity (Cifelli, 1990a, 1990b, 1990c, Cather, 2004; Eaton, 1991, 2002, 2006; Eaton and Cifelli, 2013; DeBlieux et al., 2013). Based on a wealth of previous work focused on

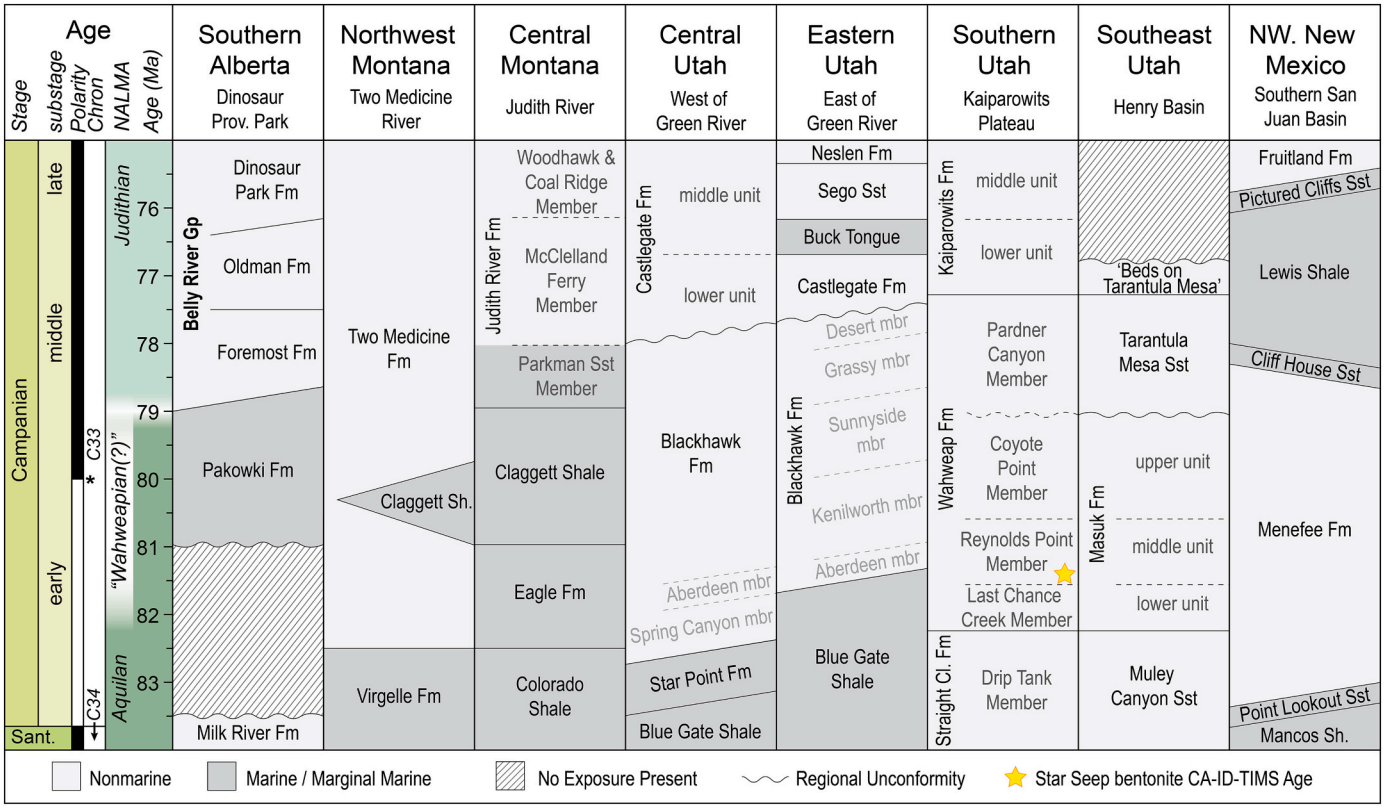

Fig. 9. Generalised temporal correlation of lower to middle Campanian strata across the Western Interior (~north to south, left to right). Geochronologic framework was adapted from Payenberg et al. (2002), Cather (2004), Cifelli et al. (2004), Roberts et al. (2005), Foreman et al. (2008), Jinnah et al. (2009), Corbett et al. (2011), Seymour and Fielding (2013), Albright and Titus (2016), Eberth (2015), Rogers et al. (2016), Fassett and Heizler (2017).

multituberculates and other microvertebrates, one hypothesis is that the Wahweap Formation contains both Aquilan and Judithian faunas that are mildly distinct from the type faunas due to either latitudinal variation or incomplete description of the type faunal assemblage. In this scenario, the Aquilan assemblage is preserved low in the Wahweap Formation, with Judithian taxa occurring higher in the formation. Alternatively, the application of a unique early to middle Campanian biochronological assemblage may be appropriate; referred to by some authors as the "Wahweapian" (Jinnah et al., 2009; Eaton and Cifelli, 2013; DeBlieux et al., 2013).

Although NALMA biochronology provides useful temporal constraint by correlating similar vertebrate assemblages using shared index taxa, radioisotopic ages are helpful as independent age constraints for correlating between temporally and latitudinally varied assemblages. The NALMA framework was developed based on northern faunal assemblages; therefore, temporal variation is difficult to untangle from latitudinal variation of southern faunal assemblages without the use of radioisotopic ages. The Aquilan faunal assemblage is described from the upper strata of the Milk River Formation in southern Alberta (Lillegraven and McKenna, 1986; Cifelli et al., 2004), which is estimated to be latest Santonian in age (~84.5 to 83.5 Ma; Payenberg et al., 2002). The type Judithian is known from the middle Campanian (~75 to 79 Ma) Judith River Formation (Rogers et al., 1993, 2016), specifically its uppermost strata (Lillegraven and McKenna, 1986; Cifelli et al., 2004). Although Cifelli et al. (2004) infer the Aquilan – Judithian transition to occur at ~79 Ma, early Campanian faunal assemblages are not preserved at either type area. This means that the unique early Campanian assemblage found in the Wahweap Formation occupies a temporal gap in sampling between classic Aquilan and Judithian assemblages and may not simply be a southern variation of either. Alternatively, the widespread application of high-precision radiometric dating techniques that facilitates these finer-scale interpretations may render strict adherence to the NALMA framework and its defined temporal intervals somewhat obsolete. Rigorous reassessment of the utility of Late Cretaceous NALMA is recommended to investigate conceptual reform from a biochronologic-centered tool to potentially a spatio-temporal model.

7. Improved chronostratigraphic constraint for fossil taxa

A refined temporal framework for vertebrate fossil from the Wahweap Formation was produced by combining our chronostratigraphic model with an updated record of localities from which in situ fossil material has been identified (Table 3, Fig. 10, Supplementary material 1). This process was conducted to explore trends in biostratigraphic zonation, and new age constraints were generated for key taxa with pre-existing stratigraphic context. It should be noted that, although well-supported, stratigraphic correlation of fossil localities to their closest measured sections then again to the Reynolds Point lectostratotype for which the Bayesian age-stratigraphic model was created will introduce minor stratigraphic uncertainties in the locality ages. These uncertainties are predicted to be significantly smaller than the Bayesian age model error envelope and thus not considered further.

7.1. Spatio-temporal distribution of vertebrates

Accepting that the less accessible, cliff-forming nature of the Pardner Canyon Member has precluded the recovery of significant non-marine vertebrate assemblages, the fossiliferous portion of the Wahweap Formation is largely restricted to the Last Chance Creek, Reynolds Point, and Coyote Point members; a temporal interval of ~3.2 million years (82.17 +1.47/-0.63 Ma to 79.00 +0.98/-0.99 Ma) (Fig. 10, Table 3). Many similar stratigraphic intervals elsewhere in the Western Interior preserve multiple, biostratigraphically-defined local faunas, including the Fruitland and Kirtland formations of northwestern New Mexico (e.g.,

Table 3
Shortlist of fossil localities from the Wahweap Formation with model ages calculated using the Bayesian age-stratigraphic model (Fig. 7, Supplementary Material 3). A complete list of fossil localities and their ages is included in Supplementary Material 1.

Museum Locality	Taxa Present (Specimen Numbers)	Area	Member	Approx. Height*	Model Age (Ma)**	2σ uncertainty +	2σ uncertainty −	Dist. from Road (m)^
UMNH VP Loc. 525	*Acristavus gaglarsoni* skull (UMNH VP 16607)	Star Seep	Reynolds Point Member	166	80.69	0.36	0.5	Moderately Close
UMNH VP Loc. 148	Centrosaurine frill (UMNH VP 9549)	Death Ridge	Coyote Point Member	313	79.00	0.98	0.99	Distal
UMNH VP Loc. 1092	*Diabloceratops eatoni* holotype, nearly complete skull (UMNH VP 16699)	Reynolds Point	Reynolds Point Member	105	81.27	0.15	0.26	Far
UMNH VP Loc. 1141	Centrosaurine frill (UMNH VP 20600)	Pilot Knoll	Last Chance Creek Member	45	81.74	1.04	0.25	Moderately Close
UMNH VP Loc. 1209	Hadrosaurid partial poscranial skeleton, partial turtle shell (UMNH VP 20213), *Melvius* tooth	Wesses Canyon	Reynolds Point Member	70	81.49	0.37	0.04	Moderately Close
UMNH VP Loc. 1212	Hadrosaurid bonebed	Tibbet Springs	Last Chance Creek Member	10	82.08	1.4	0.55	Close
UMNH VP Loc. 1276	Hadrosaurid partial skeleton	The Gut	Coyote Point Member (base)	176	80.61	0.39	0.51	Close
UMNH VP Loc. 1501	*Lythronax argestes* holotype, partial skeleton (UMNH VP 20200)	Nipple Butte	Reynolds Point Member	70	81.49	0.37	0.04	Moderately Close
UMNH VP Loc. 1654	*Machairoceratops cronusi* holotype, partial skull (UMNH VP 20550)	Star Seep	Coyote Point Member	246	80.06	0.62	0.8	Distal
UMNH VP Loc. 2994	Centrosaurine partial skull (UMNH VP 16704)	Nipple Butte	Last Chance Creek Member	50	81.69	0.94	0.2	Close
DMNH Locality 12445	Centrosaurinae gen et sp. indet (isolated element)	Nipple Butte	Last Chance Creek Member	lower	82.17 to 81.98	1.47	0.46	Close
DMNH Locality 12430	Hadrosauridae gen. et sp. indet (articulated)	Nipple Butte	Last Chance Creek Member	lower	82.17 to 81.98	1.47	0.46	Close
DMNH Locality 12431	Hadrosauridae gen. et sp. indet (partially articulated)	Nipple Butte	Last Chance Creek Member	lower	82.17 to 81.98	1.47	0.46	Close
DMNH Locality 12463	Hadrosauridae gen. et sp. indet (disarticulated)	Coyote Point	Last Chance Creek Member	lower	82.17 to 81.98	1.47	0.46	Close
DMNH Locality 6864	Pachycephalosauridae gen. et sp. nov. (DMNH EPV.131000), hadrosauridae gen. et sp. indet (disarticulated)	Brigham Plains	Last Chance Creek Member	middle	81.98 to 81.64	1.33	0.16	Close
DMNH Locality 6863	Hadrosauridae gen. et sp. indet (partially articulated)	Brigham Plains	Last Chance Creek Member	middle	81.98 to 81.64	1.33	0.16	Close
DMNH Locality 6009	Hadrosauridae gen. et sp. indet (disarticulated)	Clints Cove	Last Chance Creek Member	middle	81.98 to 81.64	1.33	0.16	Moderately Far
DMNH Locality 6006	Hadrosauridae gen. et sp. indet (disarticulated)	Clints Cove	Reynolds Point Member	middle	81.44 to 80.69	0.05	0.5	Far
DMNH Locality 12460	Hadrosauridae gen. et sp. indet (disarticulated)	Coyote Point	Coyote Point Member	lower	80.69 to 80.58	0.36	0.52	Moderately Far

* Relative to Reynolds Point lectostratotype section of Eaton (1991).
** Median model age for stratigraphic level or age range for stratigraphic intervals.
^ Direct map distance (close = 0–249 m; moderately close = 250–499 m; moderately far = 500–749 m; far = 750–999 m; distal ≥1000 m).

Sullivan and Lucas, 2003; Lucas et al., 2006), the Two Medicine and Judith River formations of Montana (e.g., Horner et al., 2001; Trexler, 2001; Mallon et al., 2016), and the Aguja Formation of West Texas (e.g., Lehman et al., 2017, 2019). Investigations of well-preserved non-marine faunas from the Campanian infer turnover rates as rapid as 600 kyr (e.g., Dinosaur Park Formation; Mallon et al., 2012), although these estimates may be influenced by preservation potential and paleoenvironmental preference (Cullen et al., 2016). Based on these examples and a temporal range of ~3.2 million years for the fossiliferous portion of the Wahweap Formation, interpretation of a single, sympatric Wahweap fauna is almost certainly over-simplistic. Though sampling of the entire fossiliferous interval across the Kaiparowits Plateau and adjacent plateaus remains incomplete, our study suggests at least a modest degree of biostratigraphic zonation within the Wahweap Formation.

Vertebrate fossils recovered from the Last Chance Creek Member (model age: 82.17 +1.47/-0.63 to 81.55 +0.62/-0.09 Ma) are largely disarticulated and durable remains from channel lag deposits. These isolated discoveries include baenid turtles, ceratopsians (e.g., UMNH VP Loc. 20600, 2994, 1141; DMNH loc. 12445), and theropods (Table 3, Supplementary material 1). Recent reconnaissance has recovered closely associated and even articulated remains in mudstone horizons largely concentrated in the lower two thirds of the member (model age: 82.17 +1.47/-0.63 to 81.76 +1.11/-0.27 Ma). This includes abundant hadrosaurid material (DMNH loc. 6863, 6864, 12430, 12431, 12463; UMNH VP Loc. 1212, 1253, 1263, 2020, 2923), a hadrosauroid skeleton (UMNH VP Loc. 2405), a pachycephalosaurid (DMNH loc. 6864), and several large crocodyliforms (UMNH VP Loc. 2587, 2999). Many of the vertebrates of the Last Chance Creek Member await full, detailed descriptions thus precluding comprehensive comparisons with other paracontemporaneous Western Interior assemblages; however, the overall composition compares closely with similar early Campanian units. This rapidly expanding Last Chance Creek Member vertebrate assemblage likely represents a unique temporal interval bridging the emerging records from the Santonian Deadhorse Coulee Member of the Milk River Formation (Evans et al., 2013), early Campanian Lower Shale Member of the Aguja Formation (Lehman et al., 2019; Prieto-Márquez et al., 2019), and Allison Member of the Menefee Formation (Lucas et al., 2005; McDonald et al., 2018; McDonald et al., 2021), although future geochronologic refinement of these units may influence faunal correlation.

Vertebrates from the Reynolds Point Member (model age: 81.55 +0.62/-0.09 to 80.61 +0.39/-0.51 Ma) are largely distributed throughout the section, mostly associated with channel lag deposits of durable skeletal material. Consisting nearly entirely of isolated remains, some specimens are exceptionally preserved, including the holotype skull of *Diabloceratops eatoni* (UMNH VP 16699), discovered in an

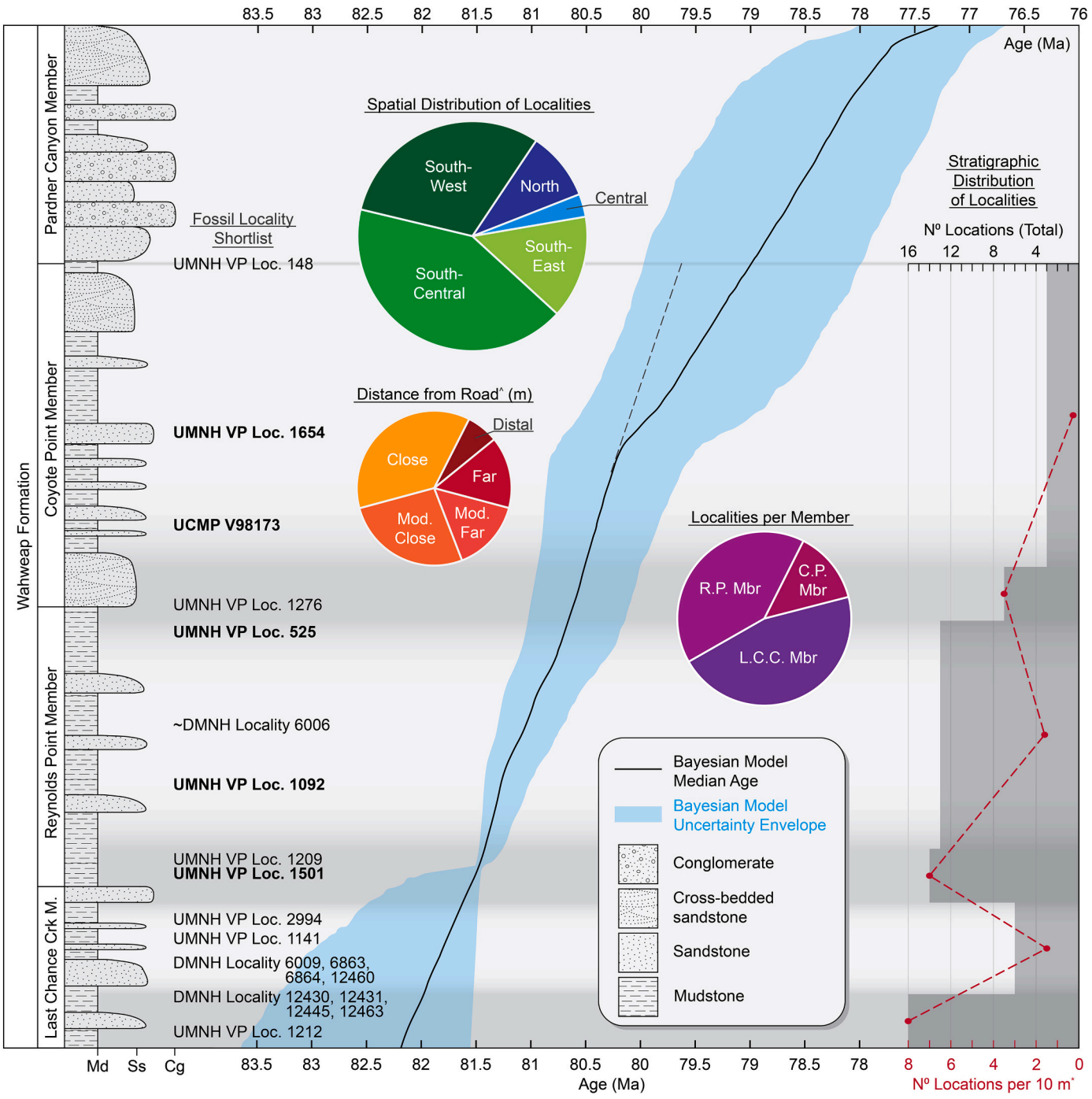

Fig. 10. Spatio-temporal distribution of fossil localities ($n = 60$). Full list of localities collated in this study can be found in Supplementary Materials 1. ^ Direct map distance. * Average stratigraphic distribution based on Reynold Point lectostratotype section. Member abbreviations: L.C.C. Mbr = Last Chance Creek Member; R.P. Mbr = Reynolds Point Member; C.P. Mbr = Coyote Point Member. See materials and methods for further detail.

indurated sandstone associated with a channel lag deposit (Kirkland and DeBlieux, 2010). Associated skeletal remains have also been recovered from mudstone horizons in the lower Reynolds Point Member, including the disarticulated and scattered skeleton of *Lythronax argestes* (UMNH VP 20200), and several hadrosaurids (e.g., UMNH VP Loc. 1209). Due to the scattered distribution of vertebrate remains throughout the Reynolds Point Member (Fig. 10), along with its still-expanding fossil record, identification of a specific faunal zone within the unit is problematic. Conversely, vertebrates from the lower portion of the Reynolds Point Member are roughly contemporaneous with the early Campanian Lower Shale Member of the Aguja Formation (Lehman et al., 2019, Prieto-Márquez et al., 2019) and Allison Member of the Menefee Formation (Lucas et al., 2005; McDonald and Wolfe, 2018), and possibly predate or partially overlap with the vertebrate assemblage from Lithofacies 3 of the Two Medicine Formation (Horner et al., 2001).

The steep exposures of the Coyote Point Member are less intensely explored than the lower members of the Wahweap Formation; however, associated remains of dinosaurs have been recovered from this unit, including the holotype of the centrosaurine ceratopsian *Machairoceratops cronusi* (UMNH VP 20550; Lund et al., 2016) and hadrosaurids (e.g., DMNH Loc. 12460) (Table 3, Supplementary material 1). A recently identified, rich lag horizon in the upper two meters of the Coyote Point

Member near Death Ridge, preserving hematite-encrusted vertebrate material, has already produced diagnostic remains of one dinosaur (Wahweap Centrosaurine C, UMNH VP 9549), in addition to abundant turtle and hadrosaurid remains, and less abundant crocodyliform and theropod material. The age of this horizon, dated to 79.03 +0.96/-1.00 Ma (Bayesian model age), or extrapolated to ~79.6 Ma based on sedimentation rates of the Reynolds Point Member, make this a significant fossiliferous interval for latitudinal comparisons with contemporaneous faunas. This includes northern faunas like those of the lower McClelland Ferry Member of the Judith River Formation (Mallon et al., 2016) and the middle of Unit 3 of the Two Medicine Formation (Horner et al., 2001). Increased sampling of this interval is necessary for more meaningful comparisons.

In summary, modest zonation of fossil localities is noted in our study including particularly rich zones in the lower two thirds of the Last Chance Creek Member, the lower levels of the Reynolds Point Member and in the uppermost Coyote Point Member (Fig. 10). The majority of fossil localities from the Wahweap Formation are situated within 500 m of a vehicle-accessible road, chiefly because access roads in the southern field areas, which encompass 87% of localities listed in this study, utilize benched areas above the steep cliff-forming Drip Tank sandstones. Despite increased accessibility to the Last Chance Creek and Reynolds Point members due to lower topographic relief and thus proximity of these exposures to roads, collection bias does not entirely explain locality distribution patterns. This is evident by the observed reduction or absence of localities in the middle to upper portion of the Last Chance Creek Member, despite abundant exposures of these levels close to roads. Increased preservation at the boundary between juxtaposing lithofacies (e.g., channel sandstones at the top of the Last Chance Creek Member to the floodplain deposits of the Reynolds Point Member) may be implicated in the observed locality distribution patters; however, detailed lithologic and taphonomic investigation is required to investigate these hypotheses further. Nevertheless, improved chronostratigraphic constraint it useful for comparing the modest faunal zones noted here with those from across the Western Interior.

7.2. Age revision for key taxa

The new high-precision U-Pb age for the Star Seep bentonite of ~81.47 Ma at the base of the Reynolds Point Member significantly improves the accuracy and precision of the inferred age of several well-known taxa including *Diabloceratops eatoni*, an early member of Ceratopsidae (Kirkland and DeBlieux, 2010; Wilson et al., 2020) and *Lythronax argestes*, one of the oldest described members of Tyrannosauridae in North America (Loewen et al., 2013a; Voris et al., 2020). As well as bearing significance in basin-scale paleontological discussion, these two taxa are ideal for discussing the revised ages because the holotype specimen of each originated from localities that were correlated with high confidence to the Reynolds Point lectostratotype section, thus the estimated ages are considered highly robust.

The holotype specimen of *Diabloceratops eatoni* was collected from a typical channel lag deposit in the Reynolds Point Member 105 m above the base of the Wahweap Formation (UMNH VP Loc. 1092) (Kirkland and DeBlieux, 2010). The age of the specimen was originally estimated to be 79.9 Ma based on $^{40}Ar/^{39}Ar$ geochronology (Jinnah et al., 2009; Kirkland and DeBlieux, 2010). Lithostratigraphic information included with the description of *D. eatoni* was indispensable in recalculating the age of the specimen. Based on the stratigraphic measurements, location description and field photographs provided by Kirkland and DeBlieux (2010), we were able to identify the exact level from which the specimen was recovered and place it with high confidence in the new chronostratigraphic model. This produced a revised age of 81.27 +0.15/-0.26 Ma for *D. eatoni*, which is 1.4 million years older than previously thought and includes quantified uncertainty. Furthermore, this revised age indicates that *Diabloceratops* is the oldest known centrosaurine, providing a key minimum age constraint for the timing of the diversification of Ceratopsidae.

Vertebrate locality UMNH VP Loc. 1501 from which the holotype *Lythronax argestes* specimen was recovered is located two meters below the Star Seep bentonite at Nipple Butte (Loewen et al., 2013a; this study). Due to this serendipitous proximity, the high-precision U-Pb age of 81.465 ± 0.036/0.042/0.097 Ma (WLS-R) tightly constrains this interval of our Bayesian age model resulting in an estimated age of 81.49 +0.37/-0.04 Ma for the L. *argestes* holotype. This model age is up to 1.6 million years older and considerably more precise than previous estimates and, furthermore, is exceptionally robust because factors such as variable sediment accumulation rates are accounted for in the Bayesian statistical approach and quantified as a component of the propagated uncertainty. This revised age for L. *argestes* (along with *Dynamoterror dynastes*, McDonald et al., 2018) provides a minimum age constraint for initial tyrannosaurid diversification given that L. *argestes* is the oldest known well-dated tyrannosaurid (Loewen et al., 2013a; Voris et al., 2020). Specifically, this even older age supports the hypothesis that tyrannosaurids diversified during a time interval that witnessed particularly high sea levels in the Western Interior (Loewen et al., 2013a).

7.3. Long distance correlation of taxa: Tyrannosaurid case example

Application of radioisotopic ages to the fossil record is of critical importance for comparing near-contemporaneous faunas, particularly across large distances; however, in doing so, the uncertainty of a radioisotopic age is just as important as the age itself. An excellent example of the utility of high-precision geochronology for distinguishing between near-contemporaneous taxa involves the holotype specimens of three of the currently oldest described tyrannosaurid dinosaurs from North America; *Lythronax argestes*, *Dynamoterror dynastes*, and *Thanatotheristes degrootorum* (Loewen et al., 2013a; McDonald et al., 2018; Voris et al., 2020). The recently described *T. degrootorum* from the Foremost Formation in Alberta, is reported to be "slightly" younger than L. *argestes* from the Wahweap Formation (Voris et al., 2020), although the age uncertainty is not reported and does not appear to have been considered. The age of the holotype specimen of *T. degrootorum* was reported as "~79.5 Ma" based on a bentonite in the Taber Coal Zone, although the origin and precision of this bentonite age is ambiguous. Considering the probable uncertainty of this data and the known uncertainty associated with the previous age of L. *argestes* (79.9 to 80.6 Ma ± 0.6 [2σ]), the two tyrannosaurs were statistically indistinguishable in age prior to new chronostratigraphic data presented herein; therefore, when *T. degrootorum* was first described, the specimen could have been considered contemporaneous with L. *argestes*, which would have significant implications for latitudinal endemism hypotheses. Conversely, the revised temporal framework for the Wahweap Formation developed herein ratifies the original statement that *T. degrootorum* is indeed quantitatively younger than L. *argestes* by approximately two million years (according to currently available data).

Reporting the limitations of available geochronologic constraint when describing new taxa reduces the likelihood of miscommunication around faunal correlations which are difficult to rectify in later work. For example, the age of the holotype specimen for *D. dynastes* from the upper Allison Member of the Menefee Formation in New Mexico (McDonald et al., 2018) remains poorly constrained due to a sparsity of dated horizons and the time-transgressive nature of Upper Cretaceous strata in the area and, as such, this specimen cannot (currently) be temporally distinguished from either L. *argestes* or *T. degrootorum*. The way in which the age of this specimen (*D. dynastes*; McDonald et al., 2018) was reported is commendably appropriate as the available chronostratigraphic data was listed and the precision was not overstated, which allows future chronostratigraphic revisions to refine the age without needing to dispute previous erroneous interpretations. These examples not only highlight the importance of the origin and uncertainty of radioisotopic ages, but also the need for higher precision chronostratigraphic data across the Upper Cretaceous strata of the

Western Interior.

8. Conclusions

This study proposes revised stratigraphic nomenclature and a robust new age model for the Wahweap Formation based on U-Pb geochronology that emphasizes quantitative uncertainty and provides comprehensive stratigraphic context for most of the archived fossil localities from the formation on the Kaiparowits Plateau. Formal recognition of members of the Wahweap Formation is intended to provide nomenclatural clarity in future work. These newly named units include, in ascending stratigraphic order, the Last Chance Creek Member, Reynolds Point Member, Coyote Point Member, and Pardner Canyon Member. These supplant the informal lower, middle, upper, and capping sandstone 'member' names of Eaton (1991). Member definitions and descriptions are primarily built upon the seminal work of Eaton (1991) and later work by Jinnah and Roberts (2011), with member boundary ages refined herein. Future regional lithostratigraphic work paired with high-precision geochronology for strata of the Markagunt and Paunsaguant Plateaus and in the Henry Basin is necessary to refine precise correlations between potentially correlative strata.

The central component of this study was the development of a new age-stratigraphic model for the Wahweap Formation that was developed using new U-Pb zircon ages and the application of Bayesian statistical modelling. The age of the base of the Wahweap Formation was determined to be ca 1.2 million years older than previously thought, and the total duration of the formation is suggested to span 82.17 +1.47/-0.63 Ma to 77.29 +0.72/-0.62 Ma. This study also compiled and stratigraphically calibrated most of the known vertebrate fossil localities discovered throughout the formation over the last 25 years. This calibrated list was used to investigate spatio-temporal trends and provide age estimates with objective uncertainties for Wahweap biota. Spatio-temporal investigation indicates that most fossil localities are situated within Last Chance Creek and Reynolds Point member strata. Whether this is due to biotic zonation or preservation bias is uncertain; however, our findings allude to the possibility of discrete faunal zonation within the formation. The second trend noted was the abundance of vertebrate localities in southern field areas (Brigham Plains to Caine Bench) compared to northern exposures on the plateau. Identification of these trends highlights possible biases and should guide future fossil exploration within the Wahweap Formation. Age calibration of currently known localities as well as future discoveries using the age model herein aids in faunal comparisons with contemporaneous biota elsewhere.

Declaration of Competing Interest

The authors declare that they have no known competing financial interests or personal relationships that could have appeared to influence the work reported in this paper.

Acknowledgements

This work was supported in part by the US National Science Foundation grant EAR1424892 to JR (S.A. Bowring). We thank the staff of Grand Staircase – Escalante National Monument and the Bureau of Land Management for issuing permits and facilitating our work. Paleontological fieldwork in the Wahweap Formation has been conducted by many groups over the past several decades, including teams of staff, students, and volunteers from the Weber State University, Utah Geological Survey, Natural History Museum of Utah/University of Utah, the Denver Museum of Nature & Science, and the Bureau of Land Management. Many projects have been supported by funds made available by the Bureau of Land Management through grants and cooperative agreements, and through generous donations by anonymous supporters. The authors also wish to thank A. Ferguson and S. Roberts for invaluable assistance during targeted lithostratigraphic field work in the Kaiparowits region.

Appendix A. Supplementary data

Supplementary data to this article can be found online at https://doi.org/10.1016/j.palaeo.2022.110876.

References

Albright, L.B., Titus, A.L., 2016. Magnetostratigraphy of Upper Cretaceous strata in Grand Staircase-Escalante National Monument, southern Utah: The Santonian-Campanian Stage boundary, reassessment of the C33N/C33R magnetochron boundary, and implications for regional sedimentation patterns within the Sevier Foreland Basin. Cretac. Res. 63, 77–94. https://doi.org/10.1016/j.cretres.2016.03.004.

Beveridge, T.L., Roberts, E.M., Titus, A.L., 2020. Volcaniclastic member of the richly fossiliferous Kaiparowits Formation reveals new insights for regional correlation and tectonics in southern Utah during the latest Campanian. Cretac. Res. 114, 104527 https://doi.org/10.1016/j.cretres.2020.104527.

Biek, R.F., Rowley, P.D., Anderson, J.J., Maldonado, F., Moore, D.W., Hacker, D.B., Eaton, J.G., Hereford, R., Sable, E.G., Filkorn, H.F., Matyjasik, B., 2015. Geologic map of the Panguitch 30′ x 60′ quadrangle, Garfield, Iron, and Kane Counties, Utah. Utah Geological Survey, Map 270DM, scale 1:62,500.

Bowring, S.A., Schoene, B., Crowley, J.L., Ramezani, J., Condon, D.J., 2006. High-precision U-Pb zircon geochronology and the stratigraphic record: Progress and promise. Paleontol. Soc. Pap. 11, 23–43. https://doi.org/10.1017/S1089332600001339.

Bowring, J.F., McLean, N.M., Bowring, S.A., 2011. Engineering cyber infrastructure for U-Pb geochronology: Tripoli and U-Pb_Redux. Geochem. Geophys. Geosyst. 12 (6) https://doi.org/10.1029/2010GC003479.

Brinkman, D.B., Newbrey, M.G., Neuman, A.G., Eaton, J.G., 2013. Freshwater osteichthyes from the Cenomanian to late Campanian of Grand Staircase-Escalante National Monument, Utah. In: Titus, A., Loewen, M. (Eds.), At the Top of the Grand Staircase: The Late Cretaceous of Southern Utah. Indiana University Press, Bloomington, pp. 195–236.

Cather, S.M., 2004. Laramide orogeny in central and northern New Mexico and southern Colorado. In: Mack, G.H., Giles, K.A. (Eds.), The Geology of New Mexico, A Geologic History: New Mexico Geological Society Special Publication, 11, pp. 203–248.

Cifelli, R.L., 1990a. Cretaceous mammals of southern Utah II. Marsupials and marsupial-like mammals from the Wahweap Formation (early Campanian). J. Vertebr. Paleontol. 10 (3), 320–331.

Cifelli, R.L., 1990b. Cretaceous mammals of southern Utah IV. Eutherian mammals from the Wahweap (Aquilan) and Kaiparowits (Judithian) formations. J. Vertebr. Paleontol. 10 (3), 346–360.

Cifelli, R.L., 1990c. A primitive higher mammal from the Late Cretaceous of southern Utah. J. Mammal. 71 (3), 343–350.

Cifelli, R.L., Eberle, J.J., Lofgren, D.L., Lillegraven, J.A., Clemens, W.A., 2004. Mammalian biochronology of the Latest Cretaceous. In: Woodburne, M.O. (Ed.), Late Cretaceous and Cenozoic Mammals of North America: Biostratigraphy and Geochronology. Columbia University Press, New York, pp. 21–42.

Clemens, W.A., 1986. Evolution of the terrestrial vertebrate fauna during the Cretaceous-Tertiary transition. In: Elliott, D.K. (Ed.), Dynamics of Extinction. John Wiley and Sons, New York, pp. 63–85.

Cobban, W.A., Walaszczyk, I., Obradovich, J.D., McKinney, K.C., 2006. A USGS zonal table for the Upper Cretaceous middle Cenomanian–Maastrichtian of the Western Interior of the United States based on ammonites, inoceramids, and radiometric ages. U.S. Geological Survey Open-File Report 2006–1250.

Condon, D.J., Schoene, B., McLean, N.M., Bowring, S.A., Parrish, R.R., 2015. Metrology and traceability of U–Pb isotope dilution geochronology (EARTHTIME tracer calibration part I). Geochim. Cosmochim. Acta 164, 464–480. https://doi.org/10.1016/j.gca.2015.05.026.

Corbett, M.J., Fielding, C.R., Birgenheier, L.P., 2011. Stratigraphy of a Cretaceous coastal-plain fluvial succession: The Campanian Masuk Formation, Henry Mountains Syncline, Utah, U.S.A. J. Sediment. Res. 81, 80–96. https://doi.org/10.2110/jsr.2011.12.

Cullen, T.M., Fanti, F., Capobianco, C., Ryan, M.J., Evans, D.C., 2016. A vertebrate microsite from a marine-terrestrial transition in the Foremost Formation (Campanian) of Alberta, Canada and the use of faunal assemblage data as a paleoenvironmental indicator. Palaeogeogr. Palaeoclimatol. Palaeoecol. 444, 101–114. https://doi.org/10.1016/j.palaeo.2015.12.015.

De Vleeschouwer, D., Parnell, A.C., 2014. Reducing time-scale uncertainty for the Devonian by integrating astrochronology and Bayesian statistics. Geology 42 (6), 491–494. https://doi.org/10.1130/G35618.1.

DeBlieux, D.D., Kirkland, J.I., Gates, T.A., Eaton, J.G., Getty, M.A., Sampson, S.D., Loewen, M.A., Hayden, M.C., 2013. Paleontological overview and taphonomy of the middle Campanian Wahweap Formation in Grand Staircase – Escalante National Monument. In: Titus, A., Loewen, M. (Eds.), At the Top of the Grand Staircase: The Late Cretaceous of Southern Utah. Indiana University Press, Bloomington, pp. 563–587.

Dickinson, W.R., Gehrels, G.E., 2008. Sediment delivery to the Cordilleran foreland basin: Insights from U-Pb ages of detrital zircons in Upper Jurassic and Cretaceous strata of the Colorado Plateau. Am. J. Sci. 308, 1041–1082.

Dickinson, W.R., Lawton, T.F., Pecha, M., Davis, S.J., Gehrels, George E., G.E., Young, R. A., 2012. Provenance of the Paleogene Colton Formation (Uinta Basin) and Cretaceous–Paleogene provenance evolution in the Utah foreland: Evidence from U-Pb ages of detrital zircons, paleocurrent trends, and sandstone petrofacies. Geosphere 8 (4), 854–880. https://doi.org/10.1130/GES00763.1.

Dodson, P.J., 1983. A faunal review of the Judith River (Oldman) Formation, Dinosaur Provincial Park, Alberta. Mosasaur 1, 89–118.

Dodson, P.J., Tatarinov, L.P., 1990. Dinosaur extinction. In: Weishampel, D.B., Dodson, P.J., Osmolska, H. (Eds.), The Dinosauria. University of California Press, Berkeley, pp. 55–62.

Doelling, H.H., 1997. Interim geologic map of the Smoky Mountain 30′ x 60′ Quadrangle, Kane and San Juan Counties, Utah and Coconino County, Arizona. In: : Utah Geological Survey, Open-File Report 359, Scale 1:100,000.

Doelling, H.H., Willis, G.C., 2006. Geologic map of the Smoky Mountain 30′ x 60′ Quadrangle, Kane and San Juan Counties, Utah and Coconino County, Arizona. In: Utah Geological Survey, Map 213, scale 1:100,000.

Doelling, H.H., Willis, G.C., 2018. Interim geologic map of the Escalante 30′ x 60′ quadrangle, Garfield and Kane Counties, Utah. In: Utah Geological Survey, Open-File Report 690DM, Scale 1:100,000.

Eaton, J.G., 1990. Stratigraphic revision of Campanian (Upper Cretaceous) rocks in the Henry Basin, Utah. Mountain Geol. 27 (1), 27–38.

Eaton, J.G., 1991. Biostratigraphic framework for the Upper Cretaceous rocks of the Kaiparowits Plateau, southern Utah. In: Nations, J., Eaton, J. (Eds.), Stratigraphy, Depositional Environments, and Sedimentary Tectonics of the Western Margin, Cretaceous Western Interior Seaway, Geological Society of America Special Paper, 260, pp. 47–63.

Eaton, J.G., 1999. Vertebrate paleontology of the Paunsaugunt Plateau, Upper Cretaceous, southwestern Utah. Utah Geological Survey Miscellaneous Publication 99-1, pp. 335–338.

Eaton, J.G., 2002. Multituberculate mammals from the Wahweap (Campanian, Aquilan) and Kaiparowits (Campanian, Judithian) formations, within and near Grand Staircase-Escalante National Monument, southern Utah. Utah Geological Survey Miscellaneous Publication 02-4 (73 p).

Eaton, J.G., 2006. Santonian (Late Cretaceous) mammals from the John Henry Member of the Straight Cliffs Formation, Grand Staircase-Escalante National Monument, Utah. J. Vertebr. Paleontol. 26 (2), 446–460. https://doi.org/10.1671/0272-4634(2006)26[446:SLCMFT]2.0.CO;2.

Eaton, J.G., Cifelli, R.L., 2013. Review of Late Cretaceous mammalian faunas of the Kaiparowits and Paunsaugunt plateaus, southwestern Utah. In: Titus, A., Loewen, M. (Eds.), At the Top of the Grand Staircase: The Late Cretaceous of Southern Utah. Indiana University Press, Bloomington, pp. 319–328.

Eaton, J.G., Cifelli, R.L., Hutchison, J.H., Kirkland, J.I., Parrish, J.M., 1999a. Cretaceous vertebrate faunas from the Kaiparowits Plateau, south-central Utah. In: Gillette, D.D. (Ed.), Vertebrate Paleontology in Utah, 99(1). Utah Geological Survey Miscellaneous Publication, pp. 345–353.

Eaton, J.G., Diem, S., Archibald, J.D., Schierup, C., Munk, H., 1999b. Vertebrate paleontology of the Upper Cretaceous rocks of the Markagunt Plateau, southwestern Utah, 99-1. Utah Geological Survey Miscellaneous Publication, pp. 323–333.

Eberth, D.A., 2005. The geology. In: Currie, P.J., Koppelhus, E.B. (Eds.), Dinosaur Provincial Park: A Spectacular Ancient Ecosystem Revealed. Indiana University Press, Bloomington, pp. 54–82.

Eberth, D.A., 2015. Origins of dinosaur bonebeds in the Cretaceous of Alberta, Canada. Can. J. Earth Sci. 52 (8), 655–681. https://doi.org/10.1139/cjes-2014-0200.

Evans, D.C., Schott, R.K., Larson, D.W., Brown, C.M., Ryan, M.J., 2013. The oldest North American pachycephalosaurid and the hidden diversity of small-bodied ornithischian dinosaurs. Nat. Commun. 4, 1828. https://doi.org/10.1038/ncomms2749.

Fassett, J.E., Heizler, M.T., 2017. An improved new age for the C33N-C32R paleomagnetic reversal, San Juan Basin, NW New Mexico and SW Colorado. In: Karlstrom, K., Gonzales, D., Zimmerer, M., Heizler, M., Ulmer-Scholle, D. (Eds.), The Geology of the Ouray-Silverton Area: 68th Annual Fall Field Conference Guidebook. New Mexico Geological Society, Socorro, pp. 115–121.

Foreman, B.Z., Rogers, R.R., Deino, A.L., Wirth, K.R., Thole, J.T., 2008. Geochemical characterization of bentonite beds in the Two Medicine Formation (Campanian, Montana), including a new $^{40}Ar/^{39}Ar$ age. Cretac. Res. 29, 373–385. https://doi.org/10.1016/j.cretres.2007.07.001.

Fricke, H.C., Foreman, B.Z., Sewall, J.O., 2010. Integrated climate model-oxygen isotope evidence for a North American monsoon during the Late Cretaceous. Earth Planet. Sci. Lett. 289, 11–21. https://doi.org/10.1016/j.epsl.2009.10.018.

Gale, A.S., Mutterlose, J., Batenburg, S., 2020. The Cretaceous Period. In: Gradstein, F. M., Ogg, J.G., Schmitz, M.D., Ogg, G.M. (Eds.), The Geologic Time Scale: Volume 2. Elsevier. https://doi.org/10.1016/C2020-1-02369-3.

Gardner, J.D., Eaton, J.G., Cifelli, R.L., 2013. Preliminary report on salamanders (Lissamphibia; Caudata) from the Late Cretaceous (late Cenomanian – late Campanian) of southern Utah, U.S.A. In: Titus, A., Loewen, M. (Eds.), At the Top of the Grand Staircase: The Late Cretaceous of Southern Utah. Indiana University Press, Bloomington, pp. 237–272.

Gates, T.A., Sampson, S.D., Zanno, L.E., Roberts, E.M., Eaton, J.G., Nydam, R.L., Hutchinson, J.H., Smith, J.A., Loewen, M.A., Getty, M.A., 2010. Biogeography of terrestrial and freshwater vertebrates from the Late Cretaceous (Campanian) Western Interior of North America. Palaeogeogr. Palaeoclimatol. Palaeoecol. 291, 371–387. https://doi.org/10.1016/j.palaeo.2010.03.008.

Gates, T.A., Horner, J.R., Hanna, R.R., Nelson, C.R., 2011. New unadorned hadrosaurine hadrosaurid (Dinosauria, Ornithopoda) from the Campanian of North America. J. Vertebr. Paleontol. 31 (4), 798–811. https://doi.org/10.1080/02724634.2011.577854.

Gates, T.A., Jinnah, Z., Levitt, C., Getty, M.A., 2014. New hadrosaurid (Dinosauria, Ornithopoda) specimens from the lower-middle Campanian Wahweap Formation of southern Utah. In: Evans, D.C. (Ed.), Hadrosaurs. Indiana University Press, Bloomington, pp. 156–173.

Gradstein, F.M., Ogg, J.G., Schmitz, M.D., Ogg, G.M., 2020. Geologic time scale 2020: volume 2. Elsevier. https://doi.org/10.1016/C2020-1-02369-3.

Gregory, H.E., Moore, R.C., 1931. The Kaiparowits Region: Geographic and geologic reconnaissance of parts of Utah and Arizona. U.S. Geological Survey Professional Paper 164 (161 p).

Hamblin, A.H., Foster, J.R., 2000. Ancient animal footprints and traces in the Grand Staircase – Escalante National Monument. In: Sprinkel, D.A., Chidsey, T.C., Anderson, P.B. (Eds.), Geology of Utah's Parks and Monuments. Utah Geological Association Publication 28.

Haq, B.U., 2014. Cretaceous eustasy revisited. Glob. Planet. Chang. 113, 44–58. https://doi.org/10.1016/j.gloplacha.2013.12.007.

Haq, B.U., Hardenbol, J., Vail, P.R., 1987. Chronology of fluctuating sea levels since the Triassic. Science 235, 1156–1166. https://doi.org/10.1126/science.235.4793.1156.

Haslett, J., Parnell, A., 2008. A simple monotone process with application to radiocarbon-dated depth chronologies. J. Royal Stat. Soc. Ser. C 57 (4), 399–418.

Herriott, T.M., Crowley, J.L., Schmitz, M.D., Wartes, M.A., Gillis, R.J., 2019. Exploring the law of detrital zircon: LA-ICP-MS and CA-TIMS geochronology of Jurassic forearc strata, Cook Inlet, Alaska, USA. Geology 47, 1044–1048. https://doi.org/10.1130/G46312.1.

Hilbert-Wolf, H.L., Simpson, E.L., Simpson, W.S., Tindall, S.E., Wizevichz, M.C., 2009. Insights into syndepositional fault movement in a foreland basin; Trends in seismites of the Upper Cretaceous, Wahweap Formation, Kaiparowits Basin, Utah, USA. Basin Res. 21, 856–871. https://doi.org/10.1111/j.1365-2117.2009.00398.x.

Hoke, G.D., Schmitz, M.D., Bowring, S.A., 2014. An ultrasonic method for isolating nonclay components from clay-rich material. Geochem. Geophys. Geosyst. 15 (2), 492–498. https://doi.org/10.1002/2013GC005125.

Holroyd, P.A., Hutchison, H., 2016. Fauna and setting of the *Adelolophus hutchisoni* type locality in the Upper Cretaceous (Campanian) Wahweap Formation of Utah. PaleoBios 33, 31196. https://doi.org/10.5070/P9331031196.

Horner, J.R., Schmitt, J.G., Jackson, F., Hanna, R., 2001. Bones and rocks of the Upper Cretaceous Two Medicine-Judith River clastic wedge complex, Montana. In: Hill, C. L. (Ed.), Field Trip Guidebook, Society of Vertebrate Paleontology 61st Annual Meeting: Mesozoic and Cenozoic Paleontology in the Western Plains and Rocky Mountains 3. Museum of the Rockies Occasional Paper, pp. 3–14.

Huang, H., Guillong, M., Hu, Y., Spandler, C., 2021. Fine tuning laser focus for improved reproducibility of U-Pb isotope analysis by LA-ICP-MS. J. Anal. At. Spectrom. 36, 836–844. https://doi.org/10.1039/d1ja00044f.

Ickert, R.B., Mundil, R., Magee Jr., C.W., Mulcahy, S.R., 2015. The U-Th-Pb systematics of zircon from the Bishop Tuff: A case study in challenges to high-precision Pb/U geochronology at the millenial scale. Geochim. Cosmochim. Acta 168, 88–110. https://doi.org/10.1016/j.gca.2015.07.018.

Irmis, R.B., Martz, J.W., Parker, W.G., Nesbitt, S.J., 2010. Re-evaluating the correlation between Late Triassic terrestrial vertebrate biostratigraphy and the GSSP-defined marine stages. Albertiana 38, 40–52.

Irmis, R.B., Hutchison, J.H., Sertich, J.J.W., Titus, A.L., 2013. Crocodyliforms from the Late Cretaceous of Grand Staircase-Escalante National Monument and vicinity, southern Utah, U.S.A. In: Titus, A., Loewen, M. (Eds.), At the Top of the Grand Staircase: The Late Cretaceous of Southern Utah. Indiana University Press, Bloomington, pp. 424–444.

Jaffey, A.H., Flynn, K.F., Glendenin, L.E., Bentley, W.C., Essling, A.M., 1971. Precision measurements of half-lives and specific activities of ^{235}U and ^{238}U. Phys. Rev. C 4 (5), 1889–1906. https://doi.org/10.1103/PhysRevC.4.1889.

Jinnah, Z.A., 2013. Tectonic and sedimentary controls, age and correlation of the Upper Cretaceous Wahweap Formation, southern Utah. In: Titus, A., Loewen, M. (Eds.), At the Top of the Grand Staircase: The Late Cretaceous of Southern Utah. Indiana University Press, Bloomington, pp. 57–73.

Jinnah, Z.A., Roberts, E.M., 2011. Facies associations, paleoenvironment, and base-level changes in the Upper Cretaceous Wahweap Formation, Utah, U.S.A. J. Sediment. Res. 81, 266–283. https://doi.org/10.2110/jsr.2011.22.

Jinnah, Z.A., Roberts, E.M., Deino, A.L., Larsen, J.S., Link, P.K., Fanning, C.M., 2009. New ^{40}Ar-^{39}Ar and detrital zircon U-Pb ages for the Upper Cretaceous Wahweap and Kaiparowits formations on the Kaiparowits Plateau, Utah: Implications for regional correlation, provenance and biostratigraphy. Cretac. Res. 30, 287–299. https://doi.org/10.1016/j.cretres.2008.07.012.

Kauffman, E.G., 1985. Cretaceous evolution of the Western Interior Basin of the United States. In: Pratt, L.M., Kauffman, E.G., Zelt, F.B. (Eds.), Fine-Grained Deposits and Biofacies of the Cretaceous Western Interior Seaway: Evidence of Cyclic Sedimentary Processes. https://doi.org/10.2110/sepmfg.04. SEPM Society for Sedimentary Geology.

Kirkland, J.I., DeBlieux, D.D., 2010. New basal centrosaurine ceratopsian skulls from the Wahweap Formation (middle Campanian), Grand Staircase – Escalante National Monument, southern Utah. In: Ryan, M.J., Chinnery-Allgeier, B.J., Eberth, D.A. (Eds.), New Perspectives on Horned Dinosaurs: The Royal Tyrell Museum Ceratopsian Symposium. Indiana University Press, Bloomington, pp. 117–140.

Kirkland, J.I., Eaton, J.G., Brinkman, D.B., 2013. Elasmobranchs from Upper Cretaceous freshwater facies in southern Utah. In: Titus, A., Loewen, M. (Eds.), At the Top of the Grand Staircase: The Late Cretaceous of Southern Utah. Indiana University Press, Bloomington, pp. 153–194.

Kuiper, K.F., Deino, A., Hilgen, F.J., Krijgsman, W., Renne, P.R., Wijbrans, J.R., 2008. Synchronizing rock clocks of earth history. Science 320, 500–504. https://doi.org/10.1126/science.1154339.

Larsen, J.S., Link, P.K., Roberts, E.M., Tapanila, L., Fanning, C.M., 2010. In: Carney, S., Tabet, D., Johnson, C. (Eds.), Cyclic Stratigraphy of the Paleogene Pine Hollow Formation and Detrital Zircon Provenance of Campanian to Eocene Sandstones of the Kaiparowits and Table Cliffs Basins, South-Central Utah, 39. Geology of South-Central Utah. Utah Geological Association Publication, pp. 194–224.

Laskowski, A.K., DeCelles, P.G., Gehrels, G.E., 2013. Detrital zircon geochronology of Cordilleran retroarc foreland basin strata, western North America. Tectonics 32, 1027–1048. https://doi.org/10.1002/tect.20065.

Lawton, T.F., Bradford, B., 2011. Correlation and provenance of Upper Cretaceous (Campanian) fluvial strata, Utah, U.S.A., from zircon U-Pb geochronology and petrography. J. Sediment. Res. 81, 495–512. https://doi.org/10.2110/jsr.2011.45.

Lawton, T.F., Pollock, S.L., Robinson, R.A.J., 2003. Integrating sandstone petrology and nonmarine sequence stratigraphy: Application to the Late Cretaceous fluvial systems of southwestern Utah, U.S.A. J. Sediment. Res. 73, 389–406. https://doi.org/10.1306/100702730389.

Lawton, T.F., Eaton, J.G., Godfrey, K.N., Schellenbach, W.L., 2014a. Compositional, paleontological and detrital-zircon data from Cretaceous strata of the Henry Mountains Basin and implications for connections with dispersal systems of Wahweap and Kaiparowits formations in southern Utah, U.S.A. In: MacLean, J.S., Biek, R.F., Huntoon, J.E. (Eds.), Geology of Utah's Far South, 43. Utah Geological Association Publication, pp. 373–396.

Lawton, T.F., Schellenbach, W.L., Nugent, A.E., 2014b. Late Cretaceous fluvial-megafan and axial river systems in the southern Cordilleran Foreland Basin: Drip Tank Member of the Straight Cliffs Formation and adjacent strata, southern Utah, U.S.A. J. Sediment. Res. 84, 407–434. https://doi.org/10.2110/jsr.2014.33.

Lehman, T.M., 1997. Late Campanian dinosaur biogeography in the Western Interior of North America. In: Wolberg, D., Stump, E. (Eds.), Dinofest International Proceedings. Philadelphia Academy of Natural Sciences, Philadelphia, pp. 223–240.

Lehman, T.M., Wick, S.L., Barnes, K.R., 2017. New specimens of horned dinosaurs from the Aguja Formation of West Texas, and a revision of *Agujaceratops*. J. Syst. Palaeontol. 15, 641–674. https://doi.org/10.1080/14772019.2016.1210683.

Lehman, T.M., Wick, S.L., Brink, A.A., Shiller, T.A., 2019. Stratigraphy and vertebrate fauna of the lower shale member of the Aguja Formation (lower Campanian) in West Texas. Cretac. Res. 99, 291–314. https://doi.org/10.1016/j.cretres.2019.02.028.

Lillegraven, J.A., McKenna, M.C., 1986. Fossil mammals from the "Mesaverde" Formation (Late Cretaceous, Judithian) of the Bighorn and Wind River basins, Wyoming, with definitions of Late Cretaceous North American land-mammal "ages". Am. Mus. Novit. 2840, 1–68.

Little, W.W., 1995. The influence of tectonics and eustasy on alluvial architecture, middle Coniacian through Campanian strata of the Kaiparowits Basin, Utah (Unpubl. Ph.D. Thesis). University of Colorado, Boulder (328 p).

Loewen, M.A., Irmis, R.B., Sertich, J.J.W., Currie, P.J., Sampson, S.D., 2013a. Tyrant dinosaur evolution tracks the rise and fall of Late Cretaceous oceans. PLoS One 8 (11). https://doi.org/10.1371/journal.pone.0079420.

Loewen, M.A., Burns, M.E., Getty, M.A., Kirkland, J.I., Vickaryous, M.K., 2013b. Review of Late Cretaceous ankylosaurian dinosaurs from the Grand Staircase region, southern Utah. In: Titus, A., Loewen, M. (Eds.), At the Top of the Grand Staircase: The Late Cretaceous of Southern Utah. Indiana University Press, Bloomington, pp. 445–462.

Loewen, M.A., Farke, A.A., Sampson, S.D., Getty, M.A., Lund, E.K., O'Connor, P.M., 2013c. Ceratopsid dinosaurs from the Grand Staircase of southern Utah. In: Titus, A., Loewen, M. (Eds.), At the Top of the Grand Staircase: The Late Cretaceous of Southern Utah. Indiana University Press, Bloomington, pp. 488–503.

Lucas, S.G., Spielmann, J.A., Braman, D.R., Brister, B.S., Peters, L., McIntosh, W.C., 2005. Age of the Cretaceous Menefee Formation, Gallina Hogback, Rio Arriba County, New Mexico. In: New Mexico Geological Society, 56th Field Conference Guidebook: Geology of the Chama Basin, pp. 231–235.

Lucas, S.G., Hunt, A.P., Sullivan, R.M., 2006. Stratigraphy and age of the Upper Cretaceous Fruitland Formation, west-central San Juan Basin, New Mexico. In: Lucas, S.G., Sullivan, R.M. (Eds.), Late Cretaceous vertebrates from the Western Interior, New Mexico Museum of Natural History and Science Bulletin, 35, pp. 1–6.

Ludwig, J.R., 2012. User's Manual for Isoplot 3.75: A Geochronological Toolkit for Microsoft Excel, 5. Berkeley Geochronology Centre Special Publication. Online version at. http://www.bgc.org/isoplot_etc/isoplot/Isoplot3_75-4_15manual.pdf.

Lund, E.K., O'Connor, P.M., Loewen, M.A., Jinnah, Z.A., 2016. A new centrosaurine ceratopsid, *Machairoceratops cronusi* gen et sp. nov., from the upper sand member of the Wahweap Formation (middle Campanian), southern Utah. PLoS One 11 (5), e0154403. https://doi.org/10.1371/journal.pone.0154403.

Mallon, J.C., Evans, D.C., Ryan, M.J., Anderson, J.S., 2012. Megaherbivorous dinosaur turnover in the Dinosaur Park Formation (upper Campanian) of Alberta, Canada. Palaeogeogr. Palaeoclimatol. Palaeoecol. 350-352, 124–138. https://doi.org/10.1016/j.palaeo.2012.06.024.

Mallon, J.C., Ott, C.J., Larson, P.L., Iuliano, E.M., Evans, D.C., 2016. *Spiclypeus shipporum* gen. et sp. nov., a boldly audacious new chasmosaurine ceratopsid (Dinosauria: Ornithischia) from the Judith River Formation (Upper Cretaceous: Campanian) of Montana, USA. PLoS One 11, e0154218. https://doi.org/10.1371/journal.pone.0154218.

Mattinson, J.M., 2005. Zircon U-Pb chemical abrasion ("CA-TIMS") method: Combined annealing and multi-step partial dissolution analysis for improved precision and accuracy of zircon ages. Chem. Geol. 220, 47–66. https://doi.org/10.1016/j.chemgeo.2005.03.011.

McDonald, A.T., Wolfe, D.G., 2018. A new nodosaurid ankylosaur (Dinosauria: Thyreophora) from the Upper Cretaceous Menefee Formation of New Mexico. PeerJ 6, e5435. https://doi.org/10.7717/peerj.5435.

McDonald, A.T., Wolfe, D.G., Dooley, A.C., 2018. A new tyrannosaurid (Dinosauria: Theropoda) from the Upper Cretaceous Menefee Formation of New Mexico. PeerJ 6, e5749. https://doi.org/10.7717/peerj.5749.

McDonald, A.T., Wolfe, D.G., Freedman-Fowler, E.A., Gates, T.A., 2021. A new brachylophosaurin (Dinosauria: Hadrosauridae) from the Upper Cretaceous Menefee Formation of New Mexico. PeerJ 9, e11084. https://doi.org/10.7717/peerj.11084.

McLean, N.M., Bowring, J.F., Bowring, S.A., 2011. An algorithm for U-Pb isotope dilution data reduction and uncertainty propagation. Geochem. Geophys. Geosyst. 12 (6) https://doi.org/10.1029/2010GC003478.

McLean, N.M., Condon, D.J., Schoene, B., Bowring, S.A., 2015. Evaluating uncertainties in the calibration of isotopic reference materials and multi-element isotopic tracers (EARTHTIME tracer calibration part II). Geochim. Cosmochim. Acta 164, 481–501. https://doi.org/10.1016/j.gca.2015.02.040.

Miall, A.D., Catuneanu, O., Vakarelov, B.K., Post, R., 2008. Chapter 9 The Western Interior Basin. In: Miall, A.D. (Ed.), Basins of the World: Volume 5. Elsevier, pp. 329–362. https://doi.org/10.1016/S1874-5997(08)00009-9.

Molenaar, C.M., Rice, D.D., 1988. Cretaceous rocks of the Western Interior Basin. In: Sloss, L.L. (Ed.), Sedimentary Cover – North American Craton. Geological Society of America D-2. https://doi.org/10.1130/DNAG-GNA-D2.

Ogg, J.G., 2012. Geomagnetic polarity time scale. In: Gradstein, F.M., Ogg, J.G., Schmitz, M.D., Ogg, G.M. (Eds.), The Geologic Time Scale 2012, 2. Elsevier BV, Oxford, UK, pp. 85–113.

Oriel, S.S., Gabrielse, H., Hay, W.W., Kottlowski, F.E., Patton, J.B., 2005. North American stratigraphic code: North American Commission on stratigraphic nomenclature. AAPG Bull. 89 (11), 1547–1591. https://doi.org/10.1306/07050504129.

Parnell, A.C., Haslett, J., Allen, J.R.M., Buck, C.E., Huntley, B., 2008. A flexible approach to assessing synchroneity of past events using Bayesian reconstructions of sedimentation history. Quat. Sci. Rev. 27 (19–20), 1872–1885. https://doi.org/10.1016/j.quascirev.2008.07.009.

Parnell, A.C., Buck, C.E., Doan, T.K., 2011. A review of statistical chronology models for high-resolution, proxy-based Holocene palaeoenvironmental reconstruction. Quat. Sci. Rev. 30, 2948–2960. https://doi.org/10.1016/j.quascirev.2011.07.024.

Payenberg, T.H.D., Braman, D.R., Davis, D.W., Miall, A.D., 2002. Litho- and chronostratigraphic relationships of the Santonian–Campanian Milk River Formation in southern Alberta and Eagle Formation in Montana utilising stratigraphy, U–Pb geochronology, and palynology. Can. J. Earth Sci. 39, 1553–1577. https://doi.org/10.1139/E02-050.

Peterson, F., 1969. Cretaceous sedimentation and tectonism in the southeastern Kaiparowits Region, Utah. U.S. Geological Survey Open-file Report, pp. 69–202. https://doi.org/10.3133/ofr69202.

Peterson, F., Waldrop, H.A., 1965. Jurassic and Cretaceous stratigraphy of south-central Kaiparowits Plateau, Utah. In: Goode, H.D., Robison, R.A. (Eds.), Geology and Resources of South-Central Utah: Utah Geological Society and Intermountain Association of Petroleum Geologists Guidebook to the Geology of Utah, 19, pp. 47–69.

Pollock, S.L., 1999. Provenance, geometry, lithofacies, and age of the Upper Cretaceous Wahweap Formation, Cordilleran Foreland Basin, southern Utah. Unpublished MSc thesis. New Mexico State University, Las Cruces (111 p).

Prieto-Márquez, A., Wagner, J.R., Lehman, T., 2019. An unusual 'shovel-billed' dinosaur with trophic specializations from the early Campanian of Trans-Pecos Texas, and the ancestral hadrosaurian crest. J. Syst. Palaeontol. 18, 1–38. https://doi.org/10.1080/14772019.2019.1625078.

Ramezani, J., Hoke, G.D., Fastovsky, D.E., Bowring, S.A., Therrien, F., Dworkin, S.I., Atchley, S.C., Nordt, L.C., 2011. High-precision U-Pb zircon geochronology of the Late Triassic Chinle Formation, Petrified Forest National Park (Arizona, USA): Temporal constraints on the early evolution of dinosaurs. GSA Bull. 123 (11/12), 2142–2159. https://doi.org/10.1130/B30433.1.

Rasmussen, C., Mundil, R., Irmis, R.B., Giesler, D., Gehrels, G.E., Olsen, P.E., Kent, D.V., Lepre, C., Kinney, S.T., Geissman, J.W., Parker, W.G., 2021. U-Pb zircon geochronology and depositional age models for the Upper Triassic Chinle Formation (Petrified Forest National Park, Arizona, USA): Implications for Late Triassic paleoecological and paleoenvironmental change. Geol. Soc. Am. Bull. 133 (3–4), 539–558. https://doi.org/10.1130/B35485.1.

Roberts, E.M., 2007. Facies architecture and depositional environments of the Upper Cretaceous Kaiparowits Formation, southern Utah. Sediment. Geol. 197, 207–233. https://doi.org/10.1016/j.sedgeo.2006.10.001.

Roberts, L.N.R., Kirschbaum, M.A., 1995. Paleogeography of the Late Cretaceous of the Western Interior of middle North America – coal distribution and sediment accumulation. U.S. Geological Survey Professional Paper 1561. https://doi.org/10.3133/pp1561, 116 p.

Roberts, E.M., Deino, A.L., Chan, M.A., 2005. $^{40}Ar/^{39}Ar$ age of the Kaiparowits Formation, southern Utah, and correlation of contemporaneous Campanian strata and vertebrate faunas along the margin of the Western Interior Basin. Cretac. Res. 26, 307–318. https://doi.org/10.1016/j.cretres.2005.01.002.

Roček, Z., Gardner, J.D., Eaton, J.G., Přikryl, T., 2013. Anuran ilia from the Upper Cretaceous of Utah – diversity and stratigraphic patterns. In: Titus, A., Loewen, M. (Eds.), At the Top of the Grand Staircase: The Late Cretaceous of Southern Utah. Indiana University Press, Bloomington, pp. 273–294.

Rogers, R.R., Swisher, C.C., Horner, J.R., 1993. $^{40}Ar/^{39}Ar$ age and correlation of the nonmarine Two Medicine Formation (Upper Cretaceous), northwestern Montana, U. S.A. Can. J. Earth Sci. 30, 1066–1075. https://doi.org/10.1139/E93-090.

Rogers, R.R., Kidwell, S.M., Deino, A.L., Mitchell, J.P., Nelson, K., Thole, J.T., 2016. Age, correlation, and lithostratigraphic revision of the Upper Cretaceous (Campanian) Judith River Formation in its type area (north-central Montana), with a comparison of low- and high-accommodation alluvial records. J. Geol. 124, 99–135. https://doi.org/10.1086/684289.

Sampson, S.D., Loewen, M.A., Farke, A.A., Roberts, E.M., Forster, C.A., Smith, J.A., Titus, A.L., 2010. New horned dinosaurs from Utah provide evidence for intracontinental dinosaur endemism. PLoS One 5 (9), e12292. https://doi.org/10.1371/journal.pone.0012292.

Sankey, J.T., 2001. Late Campanian southern dinosaurs, Aguja Formation, Big Bend, Texas. J. Paleontol. 75 (1), 208–215. https://doi.org/10.1017/S0022336000031991.

Sewall, J.O., Fricke, H.C., 2013. Andean-scale highlands in the Late Cretaceous Cordillera of the North American western margin. Earth Planet. Sci. Lett. 362, 88–98. https://doi.org/10.1016/j.epsl.2012.12.002.

Seymour, D.L., Fielding, C.R., 2013. High resolution correlation of the Upper Cretaceous stratigraphy between the Book Cliffs and the western Henry Mountains Syncline, Utah, U.S.A. J. Sediment. Res. 83, 475–494. https://doi.org/10.2110/jsr.2013.37.

Simpson, E.L., Hilbert-Wolf, H.L., Simpson, W.S., Tindall, S.E., Bernard, J.J., Jenesky, T. A., Wizevich, M.C., 2008. The interaction of aeolian and fluvial processes during deposition of the Upper Cretaceous capping sandstone member, Wahweap Formation, Kaiparowits Basin, Utah, U.S.A. Palaeogeogr. Palaeoclimatol. Palaeoecol. 270, 19–28. https://doi.org/10.1016/j.palaeo.2008.08.009.

Simpson, E.L., Koch, R., Heness, E.A., Wizevich, M.C., Tindall, S.E., Hilbert-Wolf, H.L., Golder, K., Steullet, A.K., 2014. Sedimentology and paleontology of the Upper Cretaceous Wahweap Formation sag ponds adjacent to syndepositional normal faults, Grand Staircase-Escalante National Monument, Utah. Cretac. Res. 50, 332–343. https://doi.org/10.1016/j.cretres.2014.05.001.

Sloan, R.E., 1976. The ecology of dinosaur extinction. In: Churcher, C.S. (Ed.), Essays on Palaeontology in Honour of Loris Shano Russell. University of Toronto Press, Toronto, pp. 134–155.

Sullivan, R.M., Lucas, S.G., 2003. The Kirtlandian, a new land-vertebrate "age" for the Late Cretaceous of western North America. In: New Mexico Geological Society Guidebook, 54th Field Conference: Geology of the Zuni Plateau, pp. 369–377.

Szwarc, T.S., Johnson, C.L., Stright, L.E., McFarlane, C.M., 2015. Interactions between axial and transverse drainage systems in the Late Cretaceous Cordilleran foreland basin: Evidence from detrital zircons in the Straight Cliffs Formation, southern Utah, USA. Geol. Soc. Am. Bull. 127 (3/4), 372–392. https://doi.org/10.1130/B31039.1.

Tindall, S.E., Storm, L.P., Jenesky, T.A., Simpson, E.L., 2010. Growth faults in the Kaiparowits Basin, Utah, pinpoint initial Laramide deformation in the western Colorado Plateau. Lithosphere 2 (4), 221–231. https://doi.org/10.1130/L79.1.

Titus, A.L., Loewen, M.A. (Eds.), 2013. At the Top of the Grand Staircase: The Late Cretaceous of Southern Utah. Indiana University Press, Bloomington, p. 634.

Titus, A.L., Powell, J.D., Roberts, E.M., Sampson, S.D., Pollock, S.L., Kirkland, J.I., Albright, L.B., 2005. Late Cretaceous stratigraphy, depositional environments, and macrovertebrate paleontology of the Kaiparowits Plateau, Grand Staircase – Escalante National Monument, Utah. In: Pederson, J., Dehler, C.M. (Eds.), Interior Western United States: Geological Society of America Field Guide, 6, pp. 101–128. https://doi.org/10.1130/2005.fld006(05).

Titus, A.L., Roberts, E.M., Albright, L.B., 2013. Geologic overview. In: Titus, A., Loewen, M. (Eds.), At the Top of the Grand Staircase: The Late Cretaceous of Southern Utah. Indiana University Press, Bloomington, pp. 13–41.

Titus, A.L., Eaton, J.G., Sertich, J., 2016. Late Cretaceous stratigraphy and vertebrate faunas of the Markagunt, Paunsaugunt, and Kaiparowits plateaus, southern Utah. Geol. Intermountain West 3, 229–291. https://doi.org/10.31711/giw.v3.pp229-291.

Todd, C.N., Roberts, E.M., Knutsen, E.M., Rozefelds, A.C., Huang, H., Spandler, C., 2019. Refined age and geological context of two of Australia's most important Jurassic vertebrate taxa (*Rhoetosaurus brownei* and *Siderops kehli*), Queensland. Gondwana Res. 76, 19–25. https://doi.org/10.1016/j.gr.2019.05.008.

Trayler, R.B., Schmitz, M.D., Cuitiño, J.I., Kohn, M.J., Bargo, M.S., Kay, R.F., Strömberg, C.A.E., Vizcaíno, S.F., 2020. An improved approach to age-modeling in deep time: Implication for the Santa Cruz Formation, Argentina. GSA Bull. 132 (1/2), 233–244. https://doi.org/10.1130/B35203.1.

Trexler, D., 2001. Two Medicine Formation, Montana: Geology and fauna. In: Tanke, D. H., Carpenter, K. (Eds.), Mesozoic Vertebrate Life. Indiana University Press, pp. 298–309.

Van Wagoner, J.C., Bertram, G.T., 1995. Sequence stratigraphy of foreland basin deposits: Outcrop and subsurface examples from the Cretaceous of North America. American Associate of petroleum geologists. Memoir 64. https://doi.org/10.1306/M64594 (490 p).

von Quadt, A., Gallhofer, D., Guillong, M., Peytcheva, I., Waelle, M., Sakata, S., 2014. U-Pb dating of CA/non-CA treated zircons obtained by LA-ICP-MS and CA-TIMS techniques: Impact for their geological interpretation. J. Anal. At. Spectrom. 29, 1618–1629. https://doi.org/10.1039/C4JA00102H.

Voris, J.T., Therrien, F., Zelenitsky, D.K., Brown, C.M., 2020. A new tyrannosaurine (Theropoda:Tyrannosauridae) from the Campanian Foremost Formation of Alberta, Canada, provides insight into the evolution and biogeography of tyrannosaurids. Cretac. Res. 110, 104388 https://doi.org/10.1016/j.cretres.2020.104388.

Wilson, J.P., Ryan, M.J., Evans, D.C., 2020. A new, transitional centrosaurine ceratopsid from the Upper Cretaceous Two Medicine Formation of Montana and the evolution of the '*Styracosaurus*-line' dinosaurs. R. Soc. Open Sci. 7, 200284 https://doi.org/10.1098/rsos.200284.